SIDE FORCES RESULTING FROM FORWARD-FACING STEPS AND INJECTION THROUGH A SLOT IN A SUPERSONIC FLOW

Thesis by

Wayne Robert Cooper

Flight Lieutenant

Royal Canadian Air Force

In Partial Fulfillment of the Requirements

For the Degree of

Mechanical Engineer

California Institute of Technology

Pasadena, California

1965

(Submitted May 26, 1965)

To my wife, Flo.

ACKNOWLEDGMENTS

The author wishes to express his gratitude to Professor E. E. Zukoski of the California Institute of Technology for his help and suggestions which have contributed so much to the work presented in this thesis.

Appreciation is expressed for the use of experimental data taken by Professor Zukoski and Dr. F. W. Spaid, who are also responsible for much of the original exploration and theory of the phenomenon of secondary injection.

The author would also like to thank the staff of the Supersonic Wind Tunnel of the California Institute of Technology's Graduate Aeronautical Laboratories for their assistance in the experimental portion of this research. Special thanks are due to Mr. D. J. Collins who volunteered much time, help, and advice in the operation and technique of the wind tunnel tests.

Of course, the author is deeply indebted to the Royal Canadian Air Force who have seen fit to allow and finance my work at this Institute.

Last, but not least, the author would like to express his appreciation to Roberta Duffy, whose typing ability made the final presentation of this thesis possible.

ABSTRACT

The pressure fields in front of steps and slot injections in a turbulent boundary layer were studied in an attempt to determine scaling parameters for the resulting side forces. Step and injection data of several experimenters, along with injection data taken by the author, were analyzed to determine the nature of the flow field. Observations of these studies and simplified theories led to simple dependence of the pressure field upon the variables and parameters of the flow. The step height was found to be a linear scaling parameter for the pressure field between separation and the step, and an equivalent step height with the same scaling quality was found for the injection data. A simple Mach number parameter was developed and found to be suitable for scaling the magnitude of the pressures. A graphical method based on observations of the character of the flow field was used to determine the point of separation for the injection data. The scaling parameters were applied to nitrogen and helium injection data taken at free stream Mach numbers of 2.56, 2.61, and 3.5. The results indicate that the pressure field, and hence the side force, can be suitably scaled by use of the simple parameters developed here.

TABLE OF CONTENTS

LIST OF SYMBOLS

C_d	Drag coefficient
C_f	Skin friction coefficient
$\hat{C}_f$	Local skin friction coefficient normalized by corresponding value at Re = 10^6
C_o	Orifice flow coefficient
F_s	Total side force of the pressure field $\int_0^{x_s + \Delta x_s} (P - P_\infty) \, dx$
$F_{s\,1}$	Side force contribution of separation region $\int_s^{\Delta x_s} (P - P_\infty) \, dx$
$F_{s\,2}$	Side force contribution of separated region $\int_0^{x_s} (P - P_\infty) \, dx$
h	Height of step or equivalent height caused by injectant in inches
M	Mach number
P	Static pressure
$P_{o\infty}$	Free stream total pressure
P_{oj}	Jet total pressure
Re	Reynolds number
T_j	Thrust force of the jet
X	Axial distance
X_s	Distance from the step or slot to the separation point.
ΔX_s	Distance from beginning of separation to completion of separation
Y	Vertical distance
δ	Boundary layer thickness
θ	Directional change of flow

LIST OF SYMBOLS (cont'd.)

subscripts

∞	Free stream condition
j	Injectant or jet
p	Plateau
s	Separation

I. INTRODUCTION

The work conducted here has been motivated by recent engineering application of secondary injection of gases to the design of jet flaps, jet spoilers, and thrust vector control. These devices require injection of a gas through ports or slots into a primary supersonic flow. The resulting interaction of the jet and primary flow causes a complex shock structure which interacts with and may separate the boundary layer. The result is an increase in the pressure field which causes a side force on the surface through which the injection takes place. It is attempted here to develop a practical way of predicting the induced side force caused by injection through a slot into a supersonic flow with a turbulent boundary layer.

The flow field caused by an obstacle on a surface in supersonic flow has been studied in many ways and for various reasons. The properties of the flow field are similar in many aspects, regardless of the object causing the disturbance. However, for a three-dimensional obstruction, such as an injectant issuing from a circular port, the disturbance is distinctly different from that caused by a two-dimensional object such as a step. The significant change of character is a result of the role played by the separation of the boundary layer. In the three-dimensional case, a relatively small length of the boundary layer separates, compared to the entire disturbance area. On the other hand, in the two-dimensional case, the separation of the boundary layer is the dominant feature of the flow field.

This study is concerned only with the two-dimensional case, and an attempt is made here to compare the flow fields caused by steps with those caused by injection through a slot. The disturbance caused by steps and injection will have the same general nature as that shown in Figure 1, which is a representation of the flow field taken from schlieren and shadowgraph pictures of the flow about a forward-facing step. A sketch of the typical resulting pressure field is shown as well. The flow field approximates that caused by flow over a "ramp" of some unknown shape. This imaginary "ramp" is made up of the dead air space, or recirculation region. As the flow is turned, the pressure rises. The oblique shock waves formed by the turning process interact with the boundary layer, causing it to separate in front of the "ramp." After the flow passes over the obstacle, reattachment to the wall takes place and normal flow is restored.

This schematic representation of the flow may be divided into three distinct regions: the boundary layer separation region, the separated region, and the reattachement region. Reattachment depends intimately on the type of obstruction and will not be discussed further in this work. The first two regions can be discussed, in general terms, for most types of obstacles.

Boundary layer separation takes place over a length of about two boundary layer thicknesses. In this region, the flow supports pressure gradients, both along the wall and normal to the wall. The component along the wall results from the shock structure produced by the obstacle. The normal component is due to the curvature of

the flow near the separation point, which causes the wall pressure to be higher than that near the outer edge of the boundary layer. Complete separation does not occur, in spite of the strong pressure gradients, until the local pressure is two or three times the free stream value. The high streamwise pressure gradients are illustrated in Figure 1 for the Mach 2 case.

After separation, the flow continues over the recirculation or separated region, where the boundary layer flow and the recirculating gas form a mixing region. In reality, the distinction between separation, shock waves, and mixing region is far from clear, but the regions may be idealized as being distinct. The flow in the separated region continues to be turned upward,but at a smaller rate, as the decrease in the pressure gradient on the wall indicates. A plateau pressure is reached in this region, which is about 20 per cent above the separation pressure. Finally, at the obstruction, the pressure rises to a maximum, corresponding to the bow shock wave formed by the flow impinging on the top of the obstacle.

The resulting pressure field in front of an obstacle creates a side force which is often regarded as an undesirable side effect of a necessary flow disturbance. However, this induced side force, produced by a device such as a flap, may be desirable to augment the side forces produced by the device. In some applications, the induced effects may be the primary principle of the design. Some examples of such devices are secondary injection used to produce vehicle attitude control and thrust vector control of rocket engines.

The purpose of this paper is to examine the nature of the

pressure field caused by steps, and to compare the results to pressure fields caused by injection through a slot. Much work has been done on the mechanism of separation and mixing in the flow field in front of steps, but the main interest here will be the properties of the pressure field produced. The work involving the steps will be carried out to obtain general properties of the separated flow field which can be extended to the similar disturbance caused by injecting a gas through a slot. Discussion will be restricted to two-dimensional data taken with a turbulent boundary layer.

Finally, based on the properties of the pressure field observed in the data along with simplified theories, scaling parameters will be applied to the injection data in order that side forces produced by the interaction can be predicted.

II. SEPARATION CAUSED BY STEPS

A. Description of Flow Field

Because of the amount and quality of the data available for the pressure fields caused by a forward-facing step, a survey of references 3, 4, 5, 6, 7, and 9 was carried out to establish trends of the flow field that could be generalized and applied to the similar disturbance caused by injecting gas through a slot. Because previous interest in the step data has not been directed toward the side force produced by the pressure field, this paper will emphasize the characteristics of the flow field which determine the pressure forces.

The experiments used various methods and equipment, and as a result, exact conditions were seldom duplicated. This gives a desirable, wide range of test conditions and techniques coupled with the undesirable difficulty of directly matching test data for comparison of results. Mach number and step height are important parameters in the separation process, and are easily correlated. On the other hand, the boundary layer profile, which affects the flow phenomenon, is not always determined. Even if the Reynolds number is specified, surface roughness, boundary layer trips, and methods of mounting make it practically impossible to correlate viscous effects between experiments.

Regardless of the test conditions, the flow field in front of a step is basically similar to that shown in Figure 1, displaying two distinct regions: (i) boundary layer separation region; (ii) separated region.

In the following sections, these regions will be discussed individually.

B. Boundary Layer Separation Region

In the separation region, the pressure transmitted to the wall increases abruptly until separation occurs at a pressure, P_s. These steep pressure gradients are common to turbulent boundary layer separation for a wide range of Reynolds numbers and for Mach numbers from 2 to 6. In most cases the gradients are almost identical for the same free stream conditions, regardless of the obstacle producing the separation. Once separation has been started, this region can apparently be considered independent of the process causing the disturbance. This conclusion has been maintained from the earliest observations with few restrictions or exceptions, and this phenomenon is referred to as a "free interaction region."

However, this independence does appear to apply only when the step height causing the disturbance is greater than some minimum value. Bogdonoff and Kepler[5] emphasize this restriction and estimate that if the step height is less than one and one-half the boundary layer thickness, then deviations from the "free interaction" will be observed. Observations of other experiments show similar trends. Figure 2 illustrates the change in the pressure profiles in the separation region as the step is reduced from 1.67 to 0.21 of the boundary layer thickness, δ. Note that the gradients change systematically as the step height increases from 0.21 δ to 1.25 δ. In this range of step heights, the gradient decreases with increasing h,

until finally the gradient, up to separation, becomes independent of the step height. That is, when h is greater than 1.25 δ, the separation region is a free interaction. In further discussions, only data obtained with step heights above this minimum will be referred to, unless specifically stated.

Note from Figure 2 that the distance from the beginning of the interaction to the separation point, ΔX_s, is about two and one-half boundary layer thicknesses. In the present investigation, this relationship was found to be roughly the same for the whole range of Reynolds numbers and Mach numbers studied. Table I, below, gives a brief summary of the available data and shows $\Delta X_s \approx 2.5\ \delta$. There is an indication, however, that the ratio $\Delta X_s/\delta$ decreases slightly with Mach number.

TABLE I

Reference	M_∞	h Inches	ΔX_s Inches	δ Inches	$\Delta X_s/\delta$
Sterrett and Emery[10]	5.8	0.35	0.52	0.26	2.0
	5.8	0.25	0.52	0.28	1.85
	5.5	0.35	0.51	0.23	2.23
	5.5	0.25	0.51	0.24	2.13
	4.8	0.35	0.50	0.20	2.50
	4.8	0.25	0.50	0.22	2.27
Vas and Bogdonoff[6]	3.85	0.40	0.50	0.24	2.08
	3.85	0.35	0.58	0.24	2.42
	3.85	0.30	0.53	0.24	2.21
	3.85	0.25	0.54	0.24	2.25
Bogdonoff and Kepler[5]	2.95	0.30	0.45	0.18	2.5
	2.95	0.20	0.44	0.17	2.5
	2.95	0.10	0.37	0.17	2.2
Bogdonoff[7]	2.35	0.35	0.52	0.21	2.5
	2.35	0.30	0.55	0.21	2.6
	2.35	0.25	0.47	0.21	2.2
	2.35	0.20	0.47	0.21	2.2

TABLE I (cont'd)

Reference	M_∞	h Inches	ΔX_s Inches	δ Inches	$\Delta X_s/\delta$
Bogdonoff[7]	2.35	0.15	0.47	0.21	2.2
	2.35	0.10	0.47	0.21	2.2

The static pressure on the wall at the completion of separation is referred to as the separation pressure, P_s, and has been the object of much theoretical and experimental research. The magnitude of the separation pressure depends only on the conditions of the free stream and is independent of the mechanism causing the separation. This lack of dependence on the step height appears to be maintained for all values of step height, and this result is illustrated in Figure 2. Here, the smallest h for which P_s was measured was 0.10 inches, giving a value of $h/\delta = 0.41$. Note that although the pressure gradients for this case differ from those of higher steps, the value for P_s remains virtually the same. This result appears to be generally true for the step data studied here.

A theoretical prediction of P_s was carried out by Chapman, Kuehn, and Larson[9], using a simplified analysis, and the following relationship was developed:

$$\frac{P_s - P_\infty}{P_\infty} \sim \sqrt{\hat{C}_f} \qquad (M_\infty = \text{constant}) \ . \qquad (1)$$

The term $\hat{C}_f$ is the local skin friction coefficient, normalized by its value at a Reynolds number of one million. Experimental results by the same and other workers bear out good correlation to this dependence on $\hat{C}_f$, where $\hat{C}_f$ for turbulent flow was assumed to have

the variation with Re indicated by the Karman-Schoenherr equation applicable to incompressible flow. The correlation at high Mach numbers appears to deteriorate (see Figure 3), possibly because of variations in techniques mentioned earlier.

Analysis of the pressure at separation has been attempted by several authors, and among the early suggestions of Lees[18] is probably the most direct approach. Lees suggests the following argument for laminar flows. Near the wall, the momentum equation can be approximated by

$$\frac{dP}{dx} = \left.\frac{\partial \tau}{dy}\right|_w . \tag{2}$$

Thus, from order of magnitude considerations, Lees suggests that the pressure gradient term can be approximated by $(P_s - P_\infty)/\Delta X_s$ and that the shear term can be approximated by the undisturbed shear stress divided by the undisturbed boundary layer thickness, τ/δ. Hence,

$$\frac{P_s - P_\infty}{\Delta X_s} \sim \frac{\tau}{\delta} . \tag{3}$$

The ratio $\delta/\Delta X_s$ can be eliminated from (3) by assuming that it is given by, or is proportional to, θ_s, the deflection angle of the outer edge of the boundary layer at the separation point. Substitution of this approximation and the definition $C_f = \tau/q_\infty$ into (3) gives

$$\theta_s \frac{(P_s - P_\infty)}{q_\infty} \sim C_f . \tag{4}$$

The right hand side is more easily worked with if C_f is factored to give:

$$\vartheta_s \frac{(P_s - P_\infty)}{q_\infty} = \left(\frac{C_f}{C_{fi}}\right)\hat{C}_f k_1 \quad . \tag{5}$$

Here, C_f/C_{fi} is the ratio of $C_f\{M, Re\}$ and $C_f\{0, Re\} \equiv C_{fi}$. Thus, this ratio gives the Mach number dependence of the skin friction coefficient, and $\hat{C}_f = C_f\{0, Re\}/C_f\{0, 10^6\}$ gives the Reynolds number dependence. Although relationships similar to (5) have been used for laminar flows (reference 9), this dependence on M_∞ and ϑ_s has never been included, to the author's knowledge. The term k_1 in (5) is a proportionality constant and must be evaluated experimentally.

The results of equation (5) were applied to the present work, by assuming the pressure rise, $(P_s - P_\infty)/q_\infty$, was the result of a simple, oblique shock wave caused by deflecting the flow by an angle ϑ_s. Numerical values of C_f/C_{fi} were obtained from figure 13.10, page 343, of reference 17, and the values of $\hat{C}_f$ were taken from the convenient tabulation in figure 31 of reference 9. From experimental results of Figure 3, the value of $(P_s - P_\infty)/(\sqrt{\hat{C}_f}\, q_\infty)$ at $M = 2.0$ was chosen to be 0.7. Therefore, at $M_\infty = 2.0$, and for a given Re, the value of k_1 could be determined. Hence, at this given Re, the left hand side of equation (5) could be determined at any M_∞. The appropriate ϑ_s and $(P_s - P_\infty)/q_\infty$ was obtained from oblique flow tables, and hence the variation of P_s with M_∞ was determined. Table II gives the results of the calculation for $Re = 10^6$ $(\hat{C}_f = 1)$.

Several calculations were carried out at other Reynolds numbers, and when the pressure coefficient was normalized by $\sqrt{\hat{C}_f}$, the results varied negligibly from those obtained at $Re = 10^6$. Thus, the variation of $(P_s - P_\infty)/(\sqrt{\hat{C}_f}\, q_\infty)$ resulting from equation (5) and

given in Table II is almost independent of the Reynolds number for the range $10^5 \leq Re \leq 10^7$.

TABLE II

Application of Equation (5) for $Re = 10^6$, $k_1 = 0.304$.

M_∞	C_f/C_{fi}	$(2)/k_1$	θ_s	$\Delta P/q_\infty$	$\Delta P/P_\infty$
1.5	0.84	2.76	8.3	0.330	0.60
2.0	0.76	2.50	10.0	0.250	0.70
2.5	0.67	2.04	10.0	0.200	0.88
3.0	0.60	1.98	10.7	0.184	1.16
4.0	0.47	1.55	10.8	0.145	1.62
5.0	0.37	1.22	10.2	0.120	2.10
6.0	0.30	0.99	9.8	0.101	2.55
8.0	0.22	0.73	9.0	0.080	3.58

The experimental data for separation pressure are presented in Figure 3, and they agree well with the calculated values, although the experimental results at higher M_∞ are somewhat scattered. It should be noted that the data taken by Sterrett and Emery[10] at $M_\infty = 6.3$ were possibly obtained with a transitional boundary layer.

Equation (5) can be further simplified if we assume that the oblique shocks are weak. For this case, the following approximation is valid:

$$\frac{P_s - P_\infty}{q_\infty} \approx \frac{2\theta_s}{\sqrt{M_\infty^2 - 1}} \quad . \tag{6}$$

In addition, the author has found that the Mach number dependency of C_f/C_{fi} can be approximated by

$$\frac{C_f}{C_{fi}} = \frac{k_2}{\sqrt{M_\infty^2 - 1}} \quad . \tag{7}$$

The result is a good approximation for $M_\infty > 3$, and the deviation at $M_\infty = 2.5$ is on the order of 15 per cent.

Substitution of (6) and (7) into (5) gives

$$\frac{2\theta_s^2}{\sqrt{M_\infty^2 - 1}} = \frac{k_1 k_2}{\sqrt{M_\infty^2 - 1}} \hat{C}_f \tag{8}$$

or

$$\theta_s = \sqrt{\frac{k_1 k_2}{2} \hat{C}_f} \quad . \tag{9}$$

This result indicates that the separation angle θ_s depends only on the Reynolds number, and is independent of M_∞. The remarkable results of equation (9) are substantiated by the values of θ_s in Table II, where the separation angles do not change significantly for Mach numbers between 2 and 6, a range well beyond the limits of the assumptions discussed above.

C. Separated Region

After the boundary layer separates, the pressure on the wall continues to increase, but with a decreasing gradient, until a plateau is reached. At the obstruction, the pressure climbs to a final maximum. The distinction between the plateau and the final peak is less apparent as the size of the step decreases (see Figure 2). From Figure 2, it is also obvious that at the higher step heights, the similarities of the pressure gradients continue after separation, onto the plateau, and back to the final peak. In this range of step heights, the

plateau pressure becomes independent of the step size. The breakdown of the similarity appears to occur again at $h/\delta \approx 1.25$, and hence it coincides with the change in the separation region discussed earlier. It is also seen from Figure 1 that the boundary layer increases by a factor of at least two as the flow passes over the separation region.

From the point of view of the side force induced by the pressure field, the length of the separated region, X_s, is of interest. The data of references 3, 7, 9, and 10 were examined to determine the Mach number and step height dependence of the disturbance length between the separation point and the step. The results are best illustrated in Figure 4, in which results are shown for a wide range of Mach and Reynolds numbers. These data indicate that X_s is roughly four times the step height and is virtually independent of Mach number. The data points do, however, indicate the possibility that the ratio X_s/h increases rapidly at Mach numbers less than 2.0. This constant value of X_s/h is in agreement with the almost constant values of θ_s obtained in the previous section, and shows that the geometry of the separated zone is remarkably independent of the Mach number.

The magnitude of the plateau pressure, P_p, is naturally of great importance to the side force created by an obstacle on the wall, and much work has been done in an attempt to estimate it. Theories and assumptions similar to those used for the separation pressure can also be applied to the plateau pressure. The workers of reference 9 have, in fact, used equation (1) in the form:

$$\frac{P_p - P_\infty}{P_\infty} \sim \sqrt{\hat{C}_f} \qquad (M_\infty = \text{constant}) \qquad (10)$$

and applied it to their data with reasonable success, especially at the higher Reynolds numbers. This writer examined the plateau pressures obtained by Vas and Bogdonoff[6] in a similar fashion and also found the correlation to be good for larger Reynolds numbers.

However, there is a body of data which is not correlated by equation (10). The deterioration of the correlation appears to coincide with the data obtained at low values of the ratio h/δ. When this ratio is too low, the similarities of the pressure fields observed in Figures 2 and 4 begin to break down, and the results of equation (10) seem to also deteriorate. On the other hand, when the plateau is fully developed, $\sqrt{\hat{C}_f}$ appears to be an appropriate scaling factor for the Reynolds number effects. Note, however, that the dependence on Reynolds number of equation (10) is extremely weak, and that the range of Reynolds numbers covered is not very large.

By applying equation (5) to the plateau pressure and making the simplifying assumptions of equations (6) and (7), the following approximate result is obtained.

$$\frac{P_p - P_\infty}{P_\infty} \sim \frac{M_\infty^2}{\sqrt{M_\infty^2 - 1}} \qquad (\text{Re} = \text{constant}) \qquad (11)$$

When this expression is applied to the step data, reasonable results are obtained. Because of the limited amount of data available with identical Reynolds numbers and with fully developed plateaus, a definite conclusion cannot be made. Nevertheless, the cor-

rect trend is given by (11), and the data do show that P_p is approximately proportional to the Mach number.

In summary, the present investigation has shown that the pressure profiles ahead of a step will be similar as long as h/δ is large enough. In particular, for $h/\delta > 1.3$, the pressure profiles will be identical back to the peak pressure of the separated region. The separation pressures are well correlated by equation (5) and the plateau pressures more roughly by equation (11). In keeping with the finding that θ_s is almost constant, it was shown that X_s/h was approximately constant, and roughly equal to 4.

III. SEPARATION CAUSED BY INJECTION THROUGH A SLOT

A. Experimental Details

Experimental data were taken at a Mach number of 2.56 in the 2" by $2\frac{1}{2}$" Supersonic Wind Tunnel in the Graduate Aeronautical Laboratories at the California Institute of Technology. Free stream stagnation pressure was maintained at one atmosphere, giving a test section Reynolds number of about $(2.35)(10)^5$ per inch. A fully turbulent boundary layer was ensured by means of a 0.009" wire trip attached to the nozzle block about 1.25" from the throat. Disturbances caused by the trip resulted in negligible effects in the test section. The boundary layer was approximately 0.20" thick.

Nitrogen was injected through a 0.006" slot in the wind tunnel wall, and the slot extended to within 1/4" of the sides of the tunnel. A more detailed description of the test block may be found in reference 2. Tests were conducted with the addition of brass side fences fitted flush with the ends of the slot, in an attempt to eliminate three-dimensional effects. Static pressures on the wall were measured with silicone oil manometers with a vacuum reference of about 1 millimeter of mercury. Schlieren photographs were taken for descriptive purposes only.

The injection total pressure, P_{oj}, was obtained from a pressure tap located in the plenum chamber preceding the slot. At injection pressure ratios, P_{oj}/P_{∞}, greater than 85, supersonic flow could not be maintained in the test section.

In the past, experiments with slot injection have been conducted either by injecting through the wind tunnel wall (references 1

and 2) or from a plate mounted in the test section (references 1 and 3). In both cases, the question of two-dimensional effects is a matter to be considered. It has been argued that conditions of complete two dimensionality, although seldom found in practice, are necessary for correlating and analyzing data. In Figure 6, data are shown with and without side fences, and it is clear that the effect of these fences on the pressure field is by no means insignificant. In order to standardize results, only data obtained with side fences will be discussed in this report.

In addition to the data of this present program, unanalyzed experimental results obtained by Drs. F. W. Spaid and E. E. Zukoski[1] were also used for analysis. Their data were taken at Mach numbers of 2.61, 3.5, and 4.54 by injecting through a slot in a plate mounted in the Supersonic Wind Tunnel at the Jet Propulsion Laboratory. Side fences were used, and Reynolds numbers were on the order of one million. Results of the $M_\infty = 4.54$ tests, however, are thought to have been obtained with a transitional boundary layer, and these data were weighted very lightly in this analysis. Unfortunately, boundary layer surveys were not taken during any of the tests. However, boundary layer thicknesses were estimated from shadowgraph figures and were found to be approximately 0.25" for all Mach numbers.

Data for the various Mach numbers are presented in Figures 7, 8, 9, and 10 for different injection pressure ratios and injectants. These data represent only fully turbulent boundary layers and slots with side fences attached.

Figure 5 is an enlarged shadowgraph picture illustrating the nature of the flow field created by injecting nitrogen through a slot into a free stream having $M_\infty = 2.61$. The nature of the disturbance has the same characteristics that were displayed by flow over a forward-facing step. The similarities are apparent when Figure 5 is compared to the sketch in Figure 1.

As with the disturbances caused by steps, the pressure field in front of slot injection is readily divided into the same three regions, which will be discussed in the same manner as in Part II.

B. Boundary Layer Separation Region

Figure 11 illustrates the independence of the upstream portion of the pressure field on the amount of injection causing the disturbance. Under the conditions studied here, it is reasonable to assume that the scale of the obstacle presented by injection is proportional to P_{oj}/P_∞. On this basis, we see that the "height" of the obstacle has been changed by a factor of about 8. Shadowgraph photographs, similar to the one shown in Figure 5, indicate that the lowest obstacle is about 3 times the boundary layer thickness at separation. Note, in Figure 11, that the pressure profiles for P/P_∞ less than about 2.3 are identical. Because separation was found to occur at a ratio of about 2.1 for step data at the same Mach number, it is reasonable to assume that the profiles of Figure 11 are identical up to the separation point for these data. Hence, as in the case of the steps, the separation region appears to be a free interaction region which is only affected by the free stream conditions. We can go

further, and assume that the shape of this region would also be the same if the pressure field were caused by a forward-facing step instead of by injection through a slot. This last assumption cannot be substantiated by the data presented here, since no experiments were carried out with identical free stream conditions. However, there appears to be no reason to assume otherwise at this time.

Separation pressures, P_s, were not obtained in the wind tunnel. Instead, a simplified approach was applied to the experimental data using the assumptions of the previous paragraph, and also the observation of the pressure fields caused by steps. In Part II, it was seen that the length of the separated regions, X_s, is approximately proportional to the step height. For injection, X_s was assumed to be similarly proportional to the injection pressure ratio, P_{oj}/P_∞. It was also considered that these assumptions became less valid at lower injection pressures, and therefore, these lower values were consequently weighted less than the higher ones.

With these assumptions in mind, the procedure was to measure the total disturbance length $(X_s + \Delta X_s)$ and plot these values as a function of P_{oj}/P_∞ (for given free stream conditions). A straight line was drawn through the points (according to the assumptions above), and it was assumed that extrapolation to $P_{oj}/P_\infty = 0$ gave the approximate value of ΔX_s. This value was then applied to the original data and the corresponding pressure was assumed to be P_s.

The linearity of the total disturbance length proved to be an excellent assumption, even at lower injection pressures. The values of ΔX_s obtained by this method gave separation points agreeing

reasonably well with values expected after examining separation caused by a step. The separation pressures estimated by this graphical method are also shown in Figure 3. Considering the scatter of the other data, an excellent agreement between experimental methods and this simple graphic method seems to exist.

As in the case of the steps, ΔX_s, although independent of the obstruction downstream, is dependent on M_∞ and Re. The actual dependence was not apparent from the limited range of data observed here.

C. Separated Region

From the data of Figures 7, 8, 9, and 10, it is seen that the pressure field in the separated region displays the same general character as that caused by a step. A plateau pressure is reached before a final maximum occurs near the injection point. At lower injection pressures, the plateau is not well defined, and is not distinct from the peak. The plateau value increases with increasing injector pressure, and even at the highest injection pressures this trend continues. In general, the static pressures were lower for the disturbances caused by slot injection than those caused by steps, as Figure 12 illustrates.

Using the same arguments and approximations as before, $(P_p-P_\infty)/P_\infty$ might be expected to have the same relationships as indicated by equation (10); however, not enough injection data were available to apply the factor $\sqrt{\hat{C}_f}$, since the Reynolds numbers were about the same in all experiments.

Equation (11) was applied to some of the data with good agree-

ment resulting. However, the dependence of P_p on the amount of injection restricts the direct application. That is, the plateau pressure increases with increased injection, and in the range of P_{oj}/P_∞ studied here, a constant P_p is never reached. It is not known whether a minimum P_{oj}/P_∞ (similar to the minimum h/δ for steps) can be attained, above which P_p would become constant regardless of the value of P_{oj}/P_∞. For the present, it was found that by applying equation (11) only to the data obtained at the highest injection pressures, excellent correlation is obtained. This agreement is shown in Figure 18. Although not presented in this report, the maximum deviation of all data, reduced by use of equation (11), is on the order of 10 per cent, a correlation which may be good enough for some engineering purposes.

If the length of the separated region, X_s, depends on the size of the obstacle causing the disturbance, then the changes in injection conditions should affect X_s in the same manner as changes in the height of the forward-facing step. An equivalent step height for the injection case can be found by carrying out a momentum balance in a direction parallel to the plate, on the injected material. The drag of the obstacle produced by injection is equated to the momentum flux of the injected gas which is assumed to expand to P_∞. This analysis is discussed in detail by F. W. Spaid[1] and leads to the result that the equivalent step height is given by

$$h = \frac{2C_o w}{C_d M_\infty^2} \frac{P_{oj}}{P_\infty} \frac{\gamma_j}{\gamma_\infty} \left[\left(\frac{2}{\gamma_j - 1} \right) \left(\frac{2}{\gamma_j + 1} \right)^{(\gamma_j+1)/(\gamma_j-1)} \left\{ 1 - \left(\frac{P_\infty}{P_{oj}} \right)^{(\gamma_j-1)/\gamma_j} \right\} \right]^{\frac{1}{2}} . \tag{12}$$

For the values of P_{oj}/P_{∞} used in these experiments, equation (12) gives the result that h is almost linear with the injection pressure. As was previously pointed out, X_s was found to be proportional to P_{oj}/P_{∞} ; this agreement indicates that equation (12) gives valid dependence for the injection pressure. This equivalent step height will be used as a linear scaling factor, in the same way that the height of the forward-facing step was.

The drag coefficient, C_d , appears in equation (12), and becomes important for correlating data of different Mach numbers. In reference 1, Spaid suggested two values of C_d , one based on C_p^* as defined by that writer, and one using the Prandtl-Glauert relation for linearized supersonic flow:

$$C_d = \frac{\text{constant}}{\sqrt{M_{\infty}^2 - 1}} \quad . \tag{13}$$

Examination of the flow field indicates a strong oblique shock wave at the beginning of the disturbance (Figure 5) which corresponds to the separation region. After this strong shock, only weak oblique shock waves are present in the separated region. This is substantiated by the smaller pressure gradients observed in the separated region.

It has also been shown previously that the separated region turns the flow by an angle of θ_s which is roughly 10°. The total angle that the flow is turned during the entire disturbance can be estimated by the ratio $h/X_s \approx 0.25$. This corresponds to an angle of 14°, a value which agrees with angles measured from schlieren and shadowgraph photographs of both steps and injections. It can be

concluded that the angle turned in the separated region, θ_p, is on the order of 4^o. Hence, the linearized form of C_d, as expressed in equation (13), can be justified for use in the separated region.

Therefore, this author used equation (12) with $C_d = 1/\sqrt{M_\infty^2 - 1}$ and applied it to the nitrogen injection data at various Mach numbers. Some of the results are shown in Figures 17 and 18. With the exception of $M_\infty = 4.54$ in Figure 18, which is probably transitional, the length of the separated region, X_s, is seen to be extremely well scaled by this value of h. Although only data obtained at the highest injection pressures are presented in this figure, Table III gives a summary of X_s/h for all data taken at $M_\infty = 2.56$, 2.61, and 3.5. The separation pressure is that obtained by the graphical method outlined previously.

TABLE III.

M_∞	Injectant	P_s/P_∞	X_s Inches	h Inches	X_s/h
3.5	N_2	2.07	1.88	0.740	2.54
3.5	N_2	2.07	0.99	0.357	2.77
3.5	N_2	2.07	0.52	0.178	2.91
3.5	N_2	2.07	0.21	0.084	2.51
2.61	N_2	2.0	1.57	0.674	2.23
2.61	N_2	2.0	0.88	0.339	2.58
2.61	N_2	2.0	0.38	0.169	2.24
2.56	N_2	1.8	0.88	0.371	2.37
2.56	N_2	1.8	0.47	0.194	2.43
2.56	N_2	1.8	0.24	0.0957	2.59
2.61	He	1.95	1.92	0.591	3.24
2.61	He	1.95	0.96	0.301	3.20

It can be seen from Table III that over the wide range of conditions covered, and for a given injectant, the separated region is approximately linearly dependent on the equivalent step height calculated from equation (12). An important fact to note also is that there is no definite breakdown of this scaling quality at the lower values of P_{oj}/P_{∞}. This, of course, follows from the observation that the disturbance length remains proportional to P_{oj}/P_{∞} at the smaller injection pressures. Hence, it appears that all injection data taken here differ from the step data inasmuch as the similarities of the pressure field do not break down for the smaller disturbances. The roughly constant value of X_s/h gives reason to believe that the assumptions of equations (12) and (13) give a result suitable for scaling the length of the pressure field for changes in M_{∞} and P_{oj}/P_{∞}.

However, it is seen from Table III that there is a marked difference in the values of X_s/h obtained for helium and for nitrogen. The two helium results are close to each other, but do not agree at all with the nitrogen results. It appears that the dependence of h on γ_j is not exactly that predicted by equation (12). Although the analytic model devised by Spaid[1] does not appear to permit any other expression for the momentum flux of the injectant, this author carried out a similar momentum balance, but made use of the momentum normal to the plate. In this case, the momentum flux at the slot exit was balanced with a normal component of the drag force. When use is made of equation (13), this calculation gives:

$$h' = 2C_o w \frac{\sqrt{M_{\infty}^2 - 1}}{M_{\infty}^2} \frac{P_{oj}}{P_{\infty}} \frac{\gamma_j}{\gamma_{\infty}} \left(\frac{2}{\gamma_j+1}\right)^{\gamma_j/(\gamma_j-1)} . \qquad (14)$$

The only significant difference between h and h' is the γ_j dependence. It can be shown that as γ_j increases, h decreases while h' increases. This result leads to a significant variation in the scaling qualities of the equivalent height, and the use of h' with the present data proves to be a better parameter, in spite of its questionable origin. The success of equation (14) is illustrated in Table IV, where γ_j has changed from 1.40 to 1.66 for nitrogen and helium, respectively. Only one Mach number is shown since the dependence of h and h' on M_∞ is identical.

TABLE IV.

M_∞	Injectant	P_s/P_∞	X_s Inches	h' Inches	X_s/h'
2.61	N_2	2.0	1.57	0.324	4.85
2.61	N_2	2.0	0.88	0.170	5.17
2.61	N_2	2.0	0.38	0.089	4.26
2.61	He	1.95	1.92	0.360	5.34
2.61	He	1.95	0.96	0.187	5.14

In practice, the type of gas used for injection is not usually a variable, and therefore the dependence of a scaling height with γ_j is not as important as the dependence on M_∞ and P_{oj}/P_∞. On this basis, and because so little helium data are available, h as given by equation (12) will be considered as the equivalent step height, unless otherwise specified.

In summary, it was found that for all injection pressures studied here, the nature of the pressure fields was essentially the same. The separation pressure can be roughly estimated graphically, by assuming that the disturbance length is a linear function of the

injection pressure ratio, and that the separation length, ΔX_s , is constant. These separation pressures appear to be correlated by equation (5). An equivalent step height for injection can be calculated from equations (12) and (13) that will scale the length of the separated region, X_s , in the same way as the forward-facing step height did. The value of X_s/h is about 2.5 for nitrogen injection, and about 3.4 for helium injection. If the separated regions is to be scaled for different gases injected through a slot, h' (as defined by equation (14)) appears to be a suitable parameter. The value of X_s/h' is about 5.0 . The plateau pressures increase slightly with increasing injection pressure and can be correlated quite well by equation (11).

IV. SIDE FORCE INTEGRALS

A. Side Force Due to a Forward-Facing Step

In light of the foregoing discussion, the force contribution of the separation region, defined as F_{s1}, depends only on the Mach number and Reynolds number of the flow (see Table V). Since this segment of the pressure field is small, a simplified scaling method may be used without significantly affecting the total side force. This simplification amounts to assuming ΔX_s to be constant, and using equation (6) to give

$$\frac{P-P_\infty}{P_\infty} = \frac{\gamma \theta_s M_\infty^2}{\sqrt{M_\infty^2-1}} \tag{15}$$

and by eliminating θ_s with equation (9):

$$\frac{P-P_\infty}{P_\infty} \sim \frac{M_\infty^2}{\sqrt{M_\infty^2-1}} \quad . \tag{16}$$

Equation (16) can be applied to all pressures in the separation region to scale force contribution there. At this point, we will define this contribution as F_{s1}.

For the remainder of the pressure field, from the separation point to the obstruction, the side force must be scaled by the step size. For discussion purposes, we will approximate the pressure field by a rectangle X_s inches long with a uniform pressure of P_p, and also define the contribution of this region as F_{s2}. This corresponds to assuming that the flow is turned through an angle of $\theta_s+\theta_p$ by means of a simple, oblique shock wave. The resulting side force per unit length of step is then given by:

$$F_{s2} = \left(\frac{P_p - P_\infty}{P_\infty}\right)(X_s P_\infty) \quad . \tag{17}$$

If we once again apply the small angle approximation, and at the same time normalize the side force with the step height, we get:

$$\frac{F_{s2}}{P_\infty h} \approx \frac{\gamma M_\infty^2}{\sqrt{M_\infty^2 - 1}} (\theta_s + \theta_p) \frac{X_s}{h} \quad . \tag{18}$$

To a good approximation, $h/X_s \approx \theta_s + \theta_p$, and hence:

$$\frac{F_{s2}}{P_\infty h} \approx \frac{\gamma M_\infty^2}{\sqrt{M_\infty^2 - 1}} \quad . \tag{19}$$

In the work done here, h/X_s corresponds to an angle of about 14^o, as discussed previously. It is apparent that the small angle assumption used in deriving equation (19) is not valid in these studies. However, the application of (19) to laminar data was found to give remarkably good results, since the angles given by h/X_s for laminar separation are on the order of 5^o, making the angle assumption more accurate.

In the analysis done here, the turbulent boundary layer results in angles too large for the direct application of equation (19) in predicting the scale and Mach number dependence. However, Table V shows that for a constant Mach number, the side force increases approximately linearly with step height at the higher values. This is in agreement with equation (19). Data shown in Table V are that of Vas and Bogdonoff[6] and are the same as are illustrated in Figure 2.

The dependence on the Mach number for the larger step sizes is shown in Figure 13, where the side force of the separated region,

TABLE V.

h Inches	h/δ	F_{s1}/P_∞ Inches	F_{s2}/P_∞ Inches	$F_{s2}/P_\infty h$
0.10	0.42	0.35	0.38	3.82
0.15	0.63	0.34	0.78	5.23
0.20*	0.83	0.35	1.24	6.25
0.25	1.04	0.41	1.74	6.94
0.30	1.25	0.42	2.23	7.43
0.35	1.45	0.48	2.69	7.70
0.40	1.67	0.43	3.23	8.05

F_{s2}, normalized by the product of the step height, h, and the free stream pressure, P_∞, is presented. The data show the roughly linear dependence on the Mach number as predicted by equation (19). Hence, we see that in spite of the large deflection angles, the side force, F_{s2}, displays the same h and M_∞ dependence as indicated in equation (19). This relationship can be obtained in a more convincing manner if the small angle assumption is modified to give a more realistic pressure dependence. Thus,

$$\frac{P_p - P_\infty}{P_\infty} \approx \frac{\gamma M_\infty^2}{\sqrt{M_\infty^2 - 1}} f\{\theta_s + \theta_p\} . \tag{20}$$

Since $\theta_s + \theta_p$ is approximately constant, we get:

$$\frac{F_{s2}}{P_\infty h} \sim \frac{M_\infty^2}{\sqrt{M_\infty^2 - 1}} , \tag{21}$$

or roughly,

* This value is not shown on Figure 2.

$$\frac{F_{s2}}{P_\infty h} \sim M_\infty \quad . \tag{22}$$

This relationship has been shown, in Figure 13, to be a good approximation for the range of Mach numbers studied here. It should be emphasized again that Figure 13 includes only larger values of h/δ, in accordance with the restrictions mentioned earlier. At these larger disturbances, it is interesting to note that the contribution of the separation region, F_{s1}, is relatively small.

Figure 14 shows that the total side force, $F_{s1}+F_{s2}$, can also be approximated by equation (22). This result follows from the previous observations that both ΔX_s and X_s/h are independent of M_∞ while $(P-P_\infty)/P_\infty$ has the same M_∞ variation for both regions (see equations (16) and (21)).

B. Side Force Due to Injection Through a Slot

As with a step, the force contributed by the separation region caused by injection can be scaled by the application of equation (16) to the pressures and by making use of the fact that the length ΔX_s is constant for a very wide range of conditions. Hence, F_{s1} will be constant for a given Mach number and increase linearly with M_∞. From the work done at $M_\infty = 2.61$ and 3.5, the values obtained for F_{s1}/P_∞ were roughly 0.17 and 0.21 inches, respectively. (Note that these forces are given for a unit length of slot.) These results are based on the points of separation determined by the graphical method outlined previously, and are therefore questionable. However, it is felt that these values are, at least, qualitatively correct.

The side force of the separated region will also depend on the injection conditions which determine X_s. In the case of injection, we have shown that h/X_s is constant, where h is the equivalent step height calculated from equations (12) and (13). If the same simplifying assumptions are made for the separated region as in Section A, equation (21) can be written:

$$\frac{F_{s2}}{P_\infty h} \sim \frac{M_\infty^2}{\sqrt{M_\infty^2 - 1}} \quad . \tag{23}$$

Hence, the same Mach number dependence is shown as for the step. The M_∞ range of the data studied in this analysis was not sufficient to definitely check this relationship, but the few data points available were found to indicate such a dependence. However, if we consider the expression for h, it is seen that:

$$h \sim \frac{\sqrt{M_\infty^2 - 1}}{M_\infty^2} C_o w \left(\frac{P_{oj}}{P_\infty}\right) \qquad (\gamma_j = \text{constant}) \ , \tag{24}$$

and hence the substitution of (24) into (23) gives:

$$\frac{F_{s2}}{P_\infty} \sim C_o w \left(\frac{P_{oj}}{P_\infty}\right) \qquad (\gamma_j = \text{constant}) \ . \tag{25}$$

This expression indicates that the side force caused by the disturbance is independent of the free stream Mach number and increases linearly with P_{oj}/P_∞. The application of equation (25) is shown in Figure 15, and the results indicate the validity of (25), and hence the validity of equation (23) follows.

It is interesting to apply the expression for the simplified equivalent height h'. Substitution of equation (14) into (23) gives:

$$\frac{F_{s2}}{P_\infty} \sim C_o w \left(\frac{P_{oj}}{P_\infty}\right)\left(\frac{\gamma_j}{\gamma_\infty}\right)\left(\frac{2}{\gamma_j+1}\right)^{\gamma_j/(\gamma_j-1)} . \qquad (26)$$

As before, the side force is independent of M_∞. As would be expected by the success of equation (14) in normalizing the distance X_s, equation (26) gives reasonable agreement between data with nitrogen and helium injectants, when applied to the injection data studied here. Figure 16 illustrates the correlating success of h' when applied to different injectants.

C. Normalized Side Force for Injection

One of the parameters that is of interest in engineering is the ratio of the total induced side force normalized by the thrust force of of the jet, F_s/T_j. It has been shown in the foregoing paragraphs that F_s is composed of two components, F_{s1} and F_{s2}. The behavior of these two contributions has been determined, and it was found that F_{s2} is proportional to the momentum flux and hence the thrust of the jet, T_j. The significance of this result is better illustrated by a specific example.

Let us take the results that have been found for nitrogen injection through a slot into a free stream of $M_\infty = 3.5$. The side force components for these conditions are, for $M_\infty = 3.5$,

$$F_{s1} = (0.21)\, P_\infty , \qquad (27)$$

and, from Figure 15,

$$F_{s2} \approx \left[2.4(C_o w)\frac{P_{oj}}{P_\infty}\right] P_\infty . \qquad (28)$$

The thrust of a sonic jet with injection pressure ratios greater than 16 (as is the case here) can be found, in flow tables, to

be:

$$T_j \approx 1.22\, P_{oj}\, (C_o w) \quad . \tag{29}$$

All of these values are in pounds per unit length of slot, and when the side force, F_s, is normalized by T_j, equations (27), (28), and (29) give the following results for $M_\infty = 3.5$:

$$\frac{F_s}{T_j} \approx 17.5 \left(\frac{P_\infty}{P_{oj}}\right) + 2 \, , \tag{30}$$

when the value $C_o w \approx 0.098"$ for this case has been substituted into the expression.

Equation 30 indicates that F_s/T_j approaches 2 as P_{oj}/P_∞ grows large, and increases rapidly as P_{oj}/P_∞ approaches zero. The rapid increase of F_s/T_j at low injection pressures is, of course, due to the free interaction behavior of the separation region. The asymptotic value, 2, displayed in equation (30) is independent of M_∞, since we have previously shown that F_{s2} is independent of Mach number. This is apparent when it is noted that equation (28) is found from Figure 15.

For the conditions of this example, $M_\infty = 3.5$, the two induced force terms become equal at an injection pressure ratio of about 9. For $P_{oj}/P_\infty < 9$, the contribution of the separation region becomes dominant, provided the boundary layer continues to separate.

The behavior of F_s/T_j indicated by (30) is, in fact, observed in practice. The value of this ratio reached at large P_{oj}/P_∞ is approximately 2, for all Mach numbers[3]. The rapid increase of

F_s/T_j at small P_{oj}/P_∞ is also observed, but the behavior in this range of injection pressures depends on M_∞.

In the analysis here, the dependence of M_∞ in equation (30) is included in the constant 17.5, and is a result of equation (27). A rough idea of the Mach number dependence of F_s/T_j can be shown if we assume that the force contributed by the separation region is proportional to M_∞. Hence, using the value 0.21 for $M_\infty = 3.5$, equation (27) becomes:

$$F_{s1} \approx (0.06) M_\infty P_\infty , \tag{31}$$

and consequently, equation (30) becomes:

$$\frac{F_s}{T_j} = 5 M_\infty \left(\frac{P_\infty}{P_{oj}}\right) + 2 . \tag{32}$$

Thus, the behavior of F_s/T_j for various values of M_∞ and P_{oj}/P_∞ can be, at least qualitatively, predicted by equation (32).

D. Summary and Discussion

The side force caused by the pressure field in front of an obstacle (either a forward-facing step or slot injection) can be scaled if the contributions of the separation and separated regions are considered individually. In the separation region, ΔX_s is held constant while the pressures are scaled by equation (16). The force contribution of the separated region can be scaled by the parameter h, where h is either the forward-facing step height, or the equivalent step height defined by equations (12) and (13). The side force, normalized by h, is found to be roughly linear with M_∞, as indicated by equations (21), (22), and (23).

If the simplified form of the equivalent step height, h', as defined by equation (14), is used to normalize the side force of the separated region, the results seem to agree well with equation (26). Therefore, the scaling parameter h' appears to correlate pressure fields caused by injectants of different specific heat ratios, γ_j. Once again, this normalized force is roughly linear with M_∞, as indicated by equation (23).

It would now seem possible to directly relate the equivalent step height to the actual step height, so that the side force caused by a forward-facing step could be correlated to a slot injection, or vice versa. The values of X_s/h for the two cases would seem to be a way of relating the two, but it is seen that this scales only the separated length. The plateau pressures would also have to be scaled, since it has been shown in Figure 12 that for similar disturbance lengths, the pressures associated with injection are considerably lower than with steps. Although at this time the correlation factor for the plateau pressures is not known, this writer did attempt the relationship, using $X_s/h = 4.15$ for steps and $X_s/h = 2.5$ for injection. The results indicate an error of about the same amount as the difference in the plateau pressures indicated in Figure 12. These results appear not only to substantiate the analysis done here, but also suggest that if the plateau pressures due to steps and injection can be correlated, disturbances of the two types can be related directly.

V. CONCLUSIONS

When a forward-facing step is greater than about 1.30, the boundary layer thickness, δ, the separation region can be assumed to be a free interaction region of constant length and identical pressure gradients dependent only on free stream conditions. Equation (5) is suitable for predicting the pressure at separation. When the step is greater than 1.3 δ, the length of separated region is about 4 times the step height and is independent of M_∞. The plateau pressure in this region varies approximately according to equation (11).

It was found that injection of a gas through a slot will produce the same results as the steps, except that the plateau pressures are generally lower for injection. An equivalent step height calculated by equation (12) with a drag coefficient, C_d, equal to $1/\sqrt{M_\infty^2-1}$ will effectively scale the separated region for a given injectant. This scaling quality did not break down at the lower values of h, where the force contribution of the separation becomes dominant. The value X_s/h is about equal to 2.5 and is independent of M_∞.

A more simple, but less justifiable, equivalent height can be calculated by equation (14). This value, h', appears to be effective in correlating pressure fields caused by injecting gases of different specific heat ratios, γ_j.

The side force caused by a step or slot injection increases approximately as $M_\infty^2/\sqrt{M_\infty^2-1}$, or roughly linearly with M_∞. The side force is independent of the density of the injectant, but increases with increasing specific heat ratio of the gas.

The results observed in this paper enable the pressure field in front of a step or slot injection to be scaled for various free stream and obstacle conditions. Care must be taken when the scaling is applied to injection data, because the plateau pressure increases slightly with increased injection pressures. In the range of injection pressures studied here, this error amounted to about $\pm$ 10 per cent.

A simple graphical method of determining the separation point was devised, based on observations of step data. This method was applied to the injection data with reasonable success.

The Reynolds number appears to have minor effects over the small ranges examined here, and the factor $\sqrt{\hat{C}_f}$ seems to be a suitable correlating parameter.

REFERENCES

1. F. W. Spaid: "A Study of Secondary Injection of Gases into a Supersonic Flow," Ph.D. Thesis, California Institute of Technology (June 1964).

2. H. W. Burden: "Some Effects of Secondary Injection of Gases into a Supersonic Flow," A. E. Thesis, California Institute of Technology (June 1964).

3. A. Heyser and F. Maurer: "Experimental Investigations on Solid Spoilers and Jet Spoilers at Mach Numbers of 0.6 to 2.8," Jet Propulsion Laboratory Translation No. 32 (21 February 1964).

4. S. M. Bogdonoff, C. E. Kepler and E. Sanlorenzo: "A Study of Shock Wave Turbulent Boundary Layer Interaction at M = 3," Princeton University Report No. 222 (July 1953).

5. S. M. Bogdonoff and C. E. Kepler: "Separation of a Supersonic Turbulent Boundary Layer," Princeton University Report No. 249 (January 1954).

6. I. E. Vas and S. M. Bogdonoff: "Interaction of a Turbulent Boundary Layer with a Step at M = 3.85," Princeton University Report No. 295 (April 1955).

7. Seymour M. Bogdonoff: "Some Experimental Studies of the Separation of Supersonic Turbulent Boundary Layers," Princeton University Report No. 336 (June 1955).

8. Dean R. Chapman, Donald M. Kuehn, and Howard K. Larson: "Preliminary Report on a Study of Separated Flows in Supersonic and Subsonic Streams," NACA RM A55L14 (June 1956).

9. Dean R. Chapman, Donald M. Kuehn, and Howard K. Larson: "Investigation of Separated Flows in Supersonic and Subsonic Streams with Emphasis on the Effect of Transition," NACA TN 3869 (March 1957).

10. James R. Sterrett and James C. Emery: "Extension of Boundary Layer Separation Criteria to a Mach Number of 6.5 by utilizing Flat Plates with Forward Facing Steps," NASA TN D-618 (December 1960).

11. Roy H. Lange: "Present Status of Information Relative to the Prediction of Shock-Induced Boundary Layer Separation," NACA TN 3065 (February 1954).

12. W. E. Moeckel: "Flow Separation Ahead of a Blunt Axially Symmetric Body at Mach Numbers 1.76 to 2.10," NACA RM E51125 (December 1951).

13. Luigi Crocco and Ronald F. Probstein: "The Peak Pressure Rise Across and Oblique Shock Emerging from a Turbulent Boundary-Layer over a Plane Surface," Princeton University Report No. 254 (March 1954).

14. Eugene S. Love: "Pressure Rise Associated with Shock-Induced Boundary-Layer separation," NACA TN 3601 (December 1955).

15. Coleman duP. Donaldson and Roy H. Lange: "Study of the Pressure Rise Across Shock Waves Required to Separate Laminar and Turbulent Boundary-Layers," NACA TN 2770 (September 1952).

16. Gadd, Holder and Regan: "An Experimental Investigation of the Interaction Between Shock Waves and Boundary Layers," Proceedings of Royal Society of London, Serial A, Vol. 226, 1954, Pages 227-253.

17. H. W. Liepmann and A. Roshko: "Elements of Gasdynamics," GALCIT Aeronautical Series, John Wiley & Sons.

18. Lester Lees: "Interaction Between the Laminar Boundary Layer over a Plane Surface and an Incident Oblique Shock Wave," Report 143, Princeton University, Aeronautical Engineering Laboratory (January 1949).

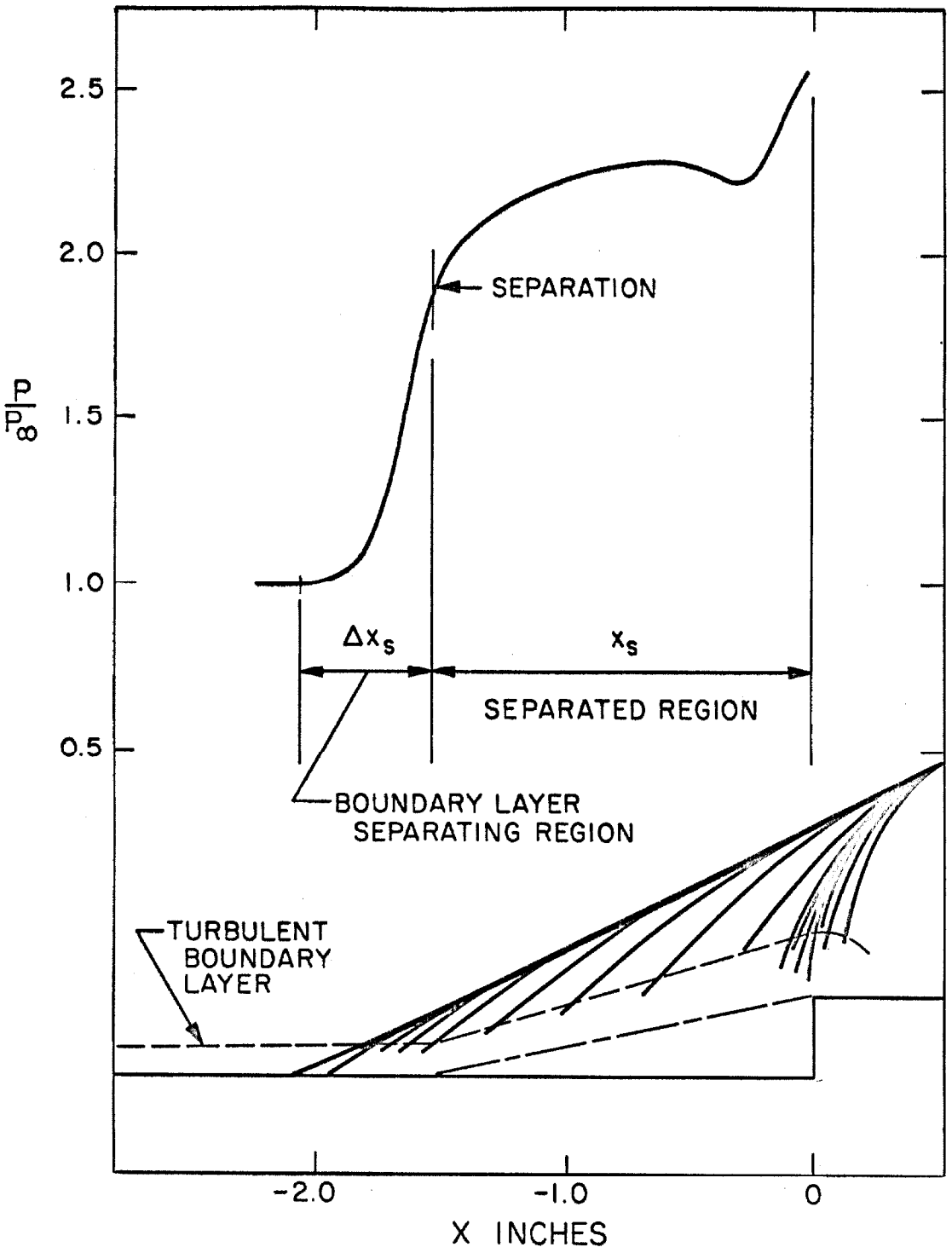

Figure 1. Sketch of Flow and Pressure Fields Created by a Step of 0.35 Inches in a Mach 2.0 Stream.

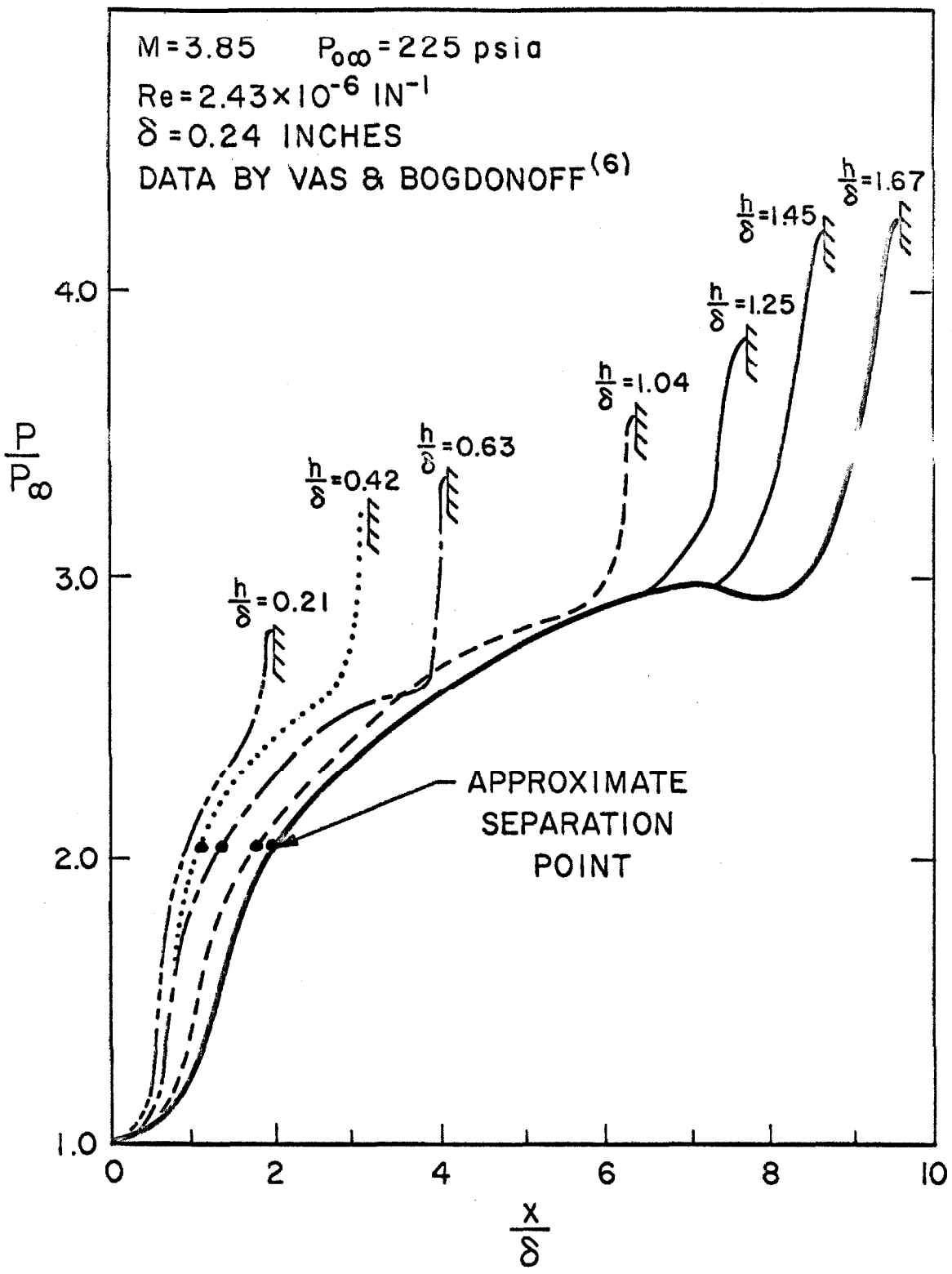

Figure 2. Variation of Pressure Field with Ratio of Step Height to Boundary Layer Thickness.

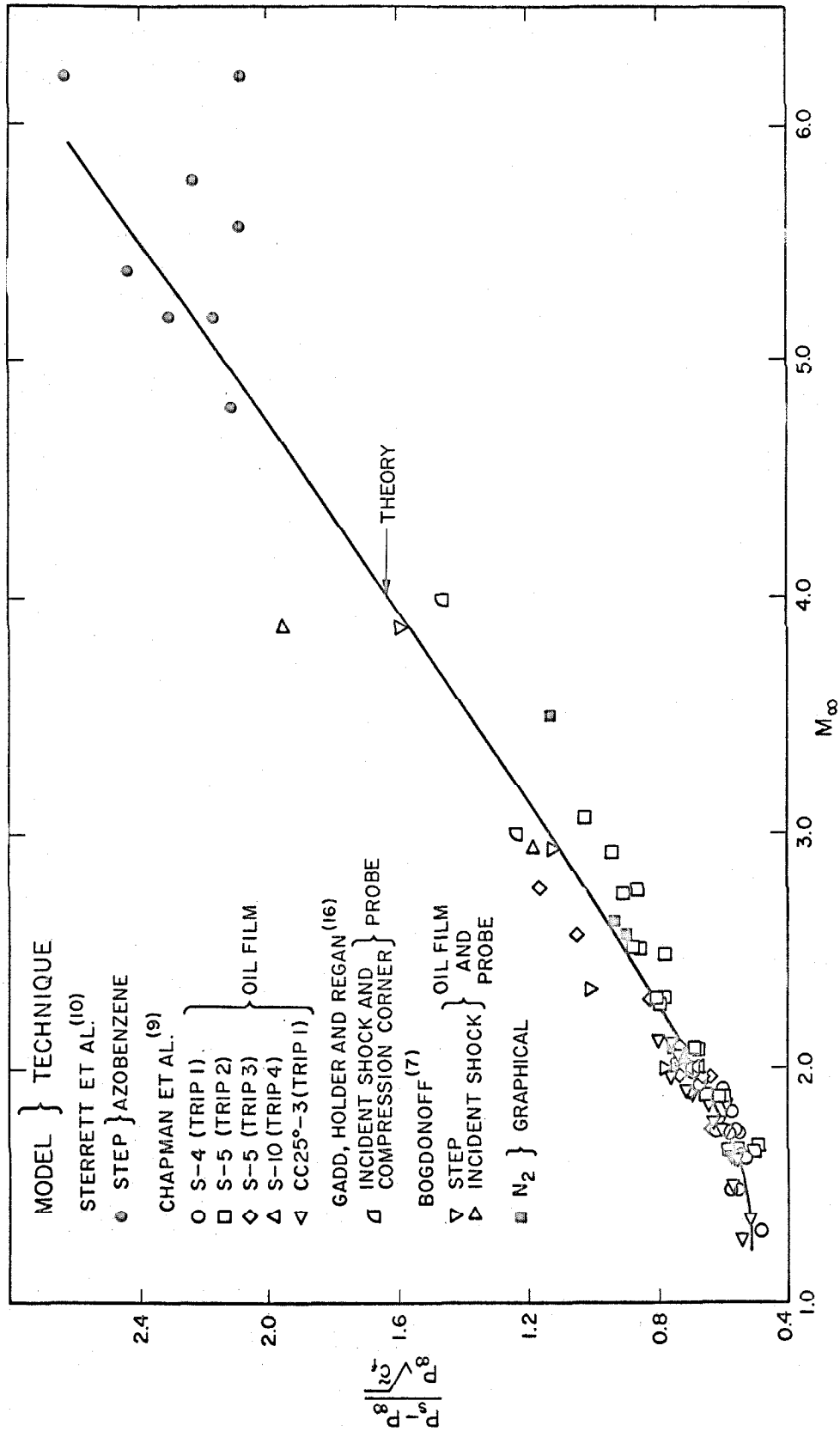

Figure 3: Separation Pressures, Correlated by $\sqrt{\tilde{c}_f}$, for Various Conditions and Determined by Various Techniques.

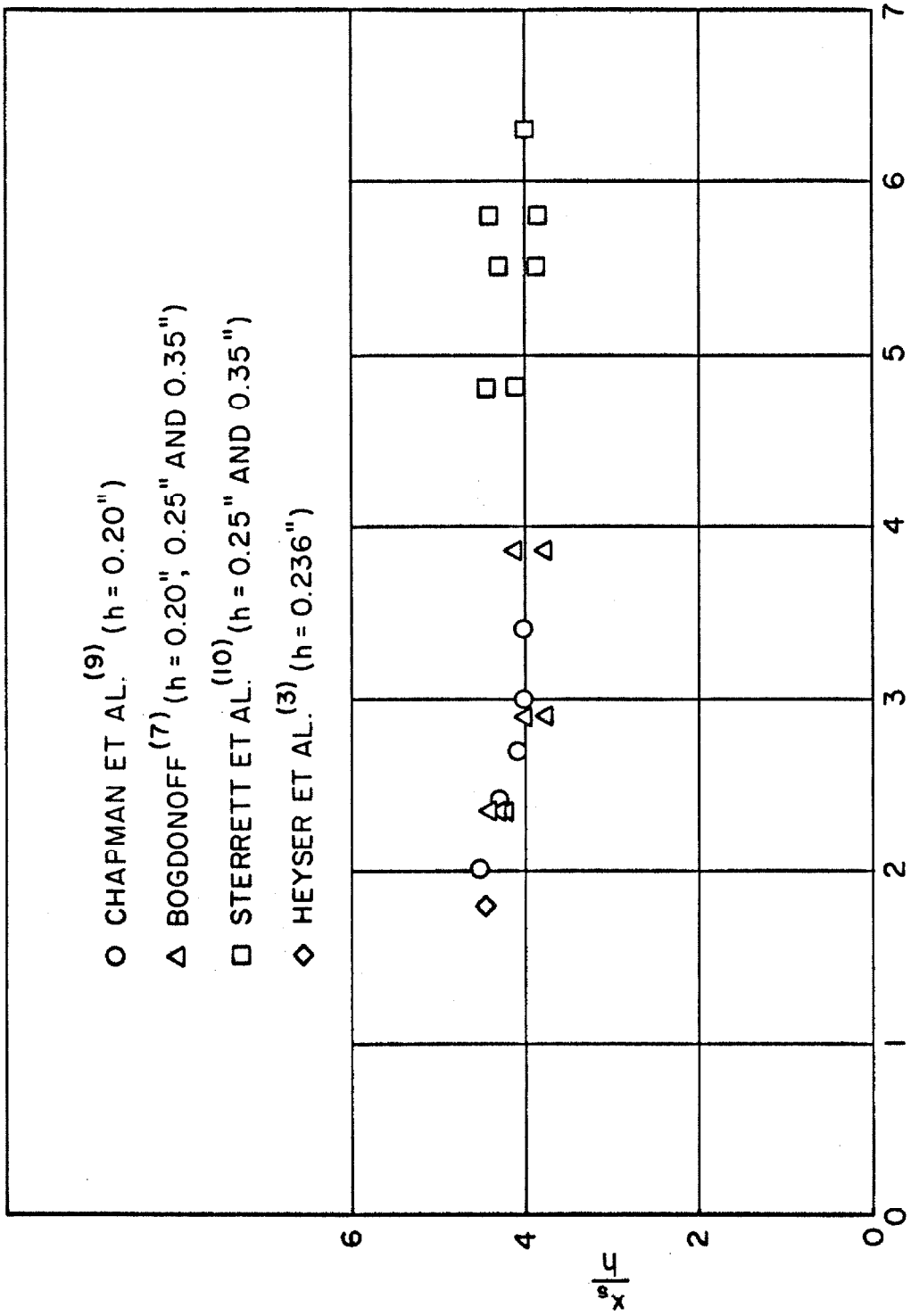

Figure 4. Dependence of Separation Distance on Mach Number and Step Height.

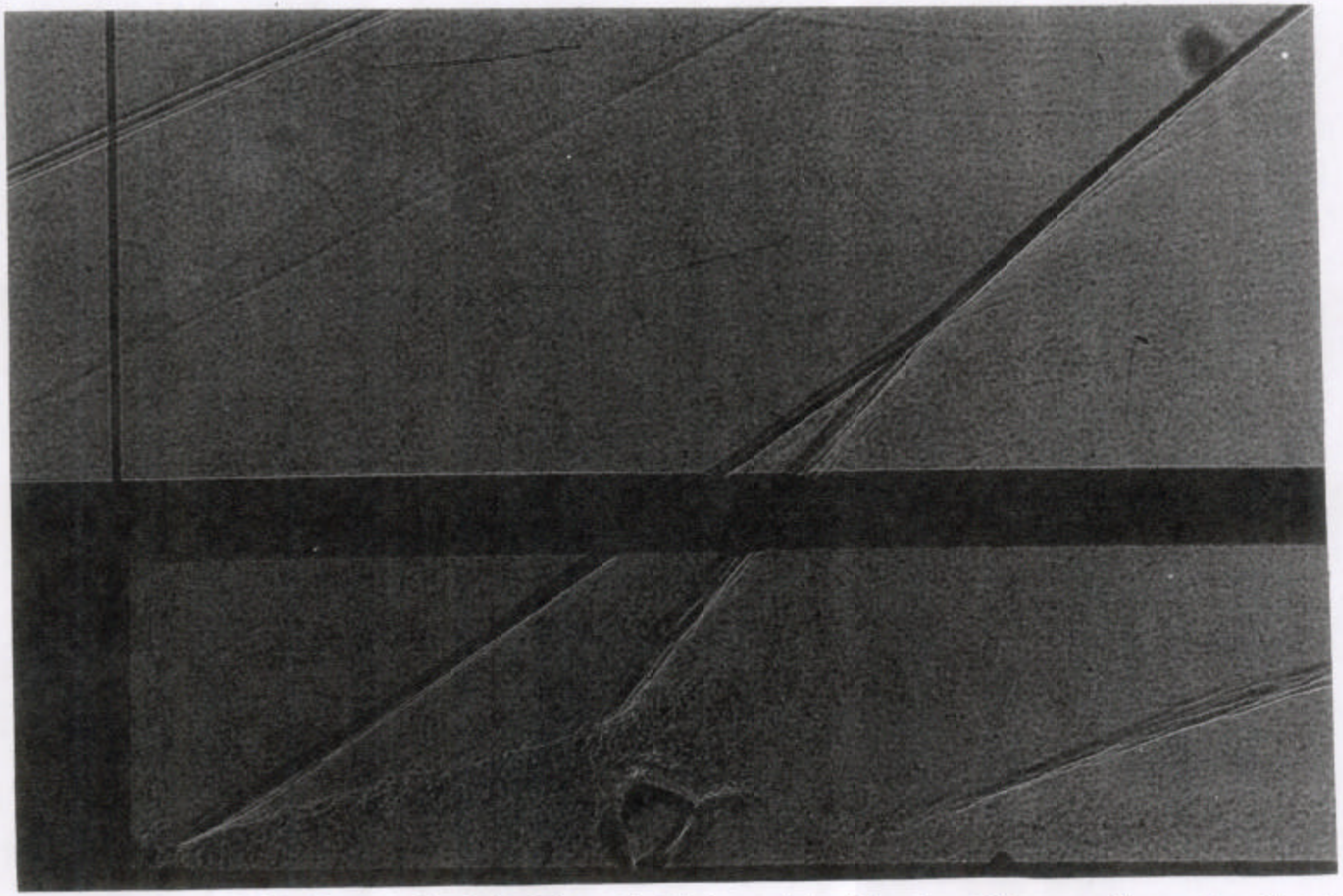

Figure 5. Enlarged Shadowgraph of the Flow Field Caused by Injecting Nitrogen Through a Slot in a Plate, with $M_{\infty} = 2.61$, $P_{oj}/P_{\infty} = 85.8$, and $Re \approx 10^6$. (Scale: 1" = 0.639".)

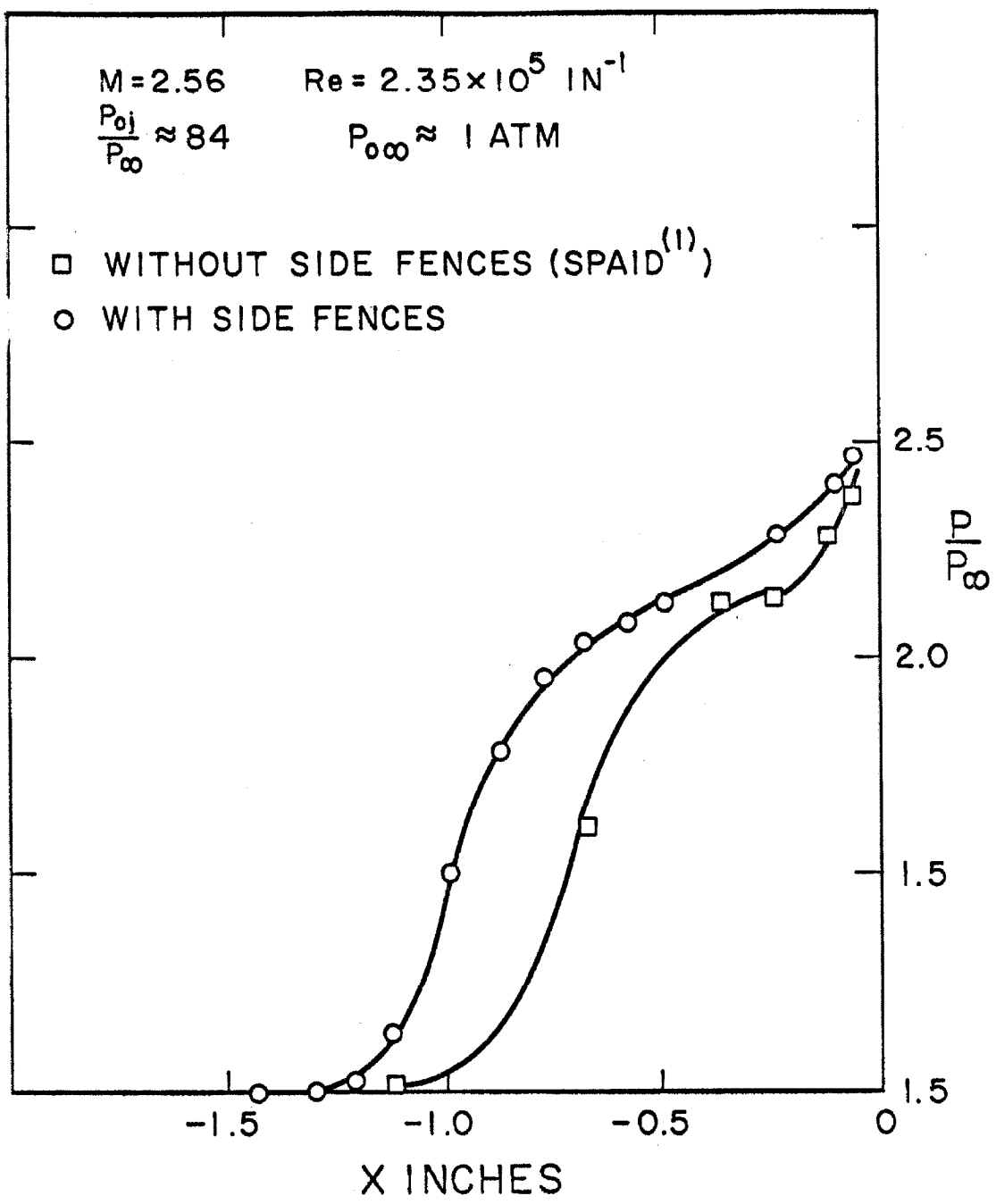

Figure 6. Effects of Side Fences on Pressure Field Caused by Injecting Nitrogen Through a Slot at $M_\infty = 2.56$.

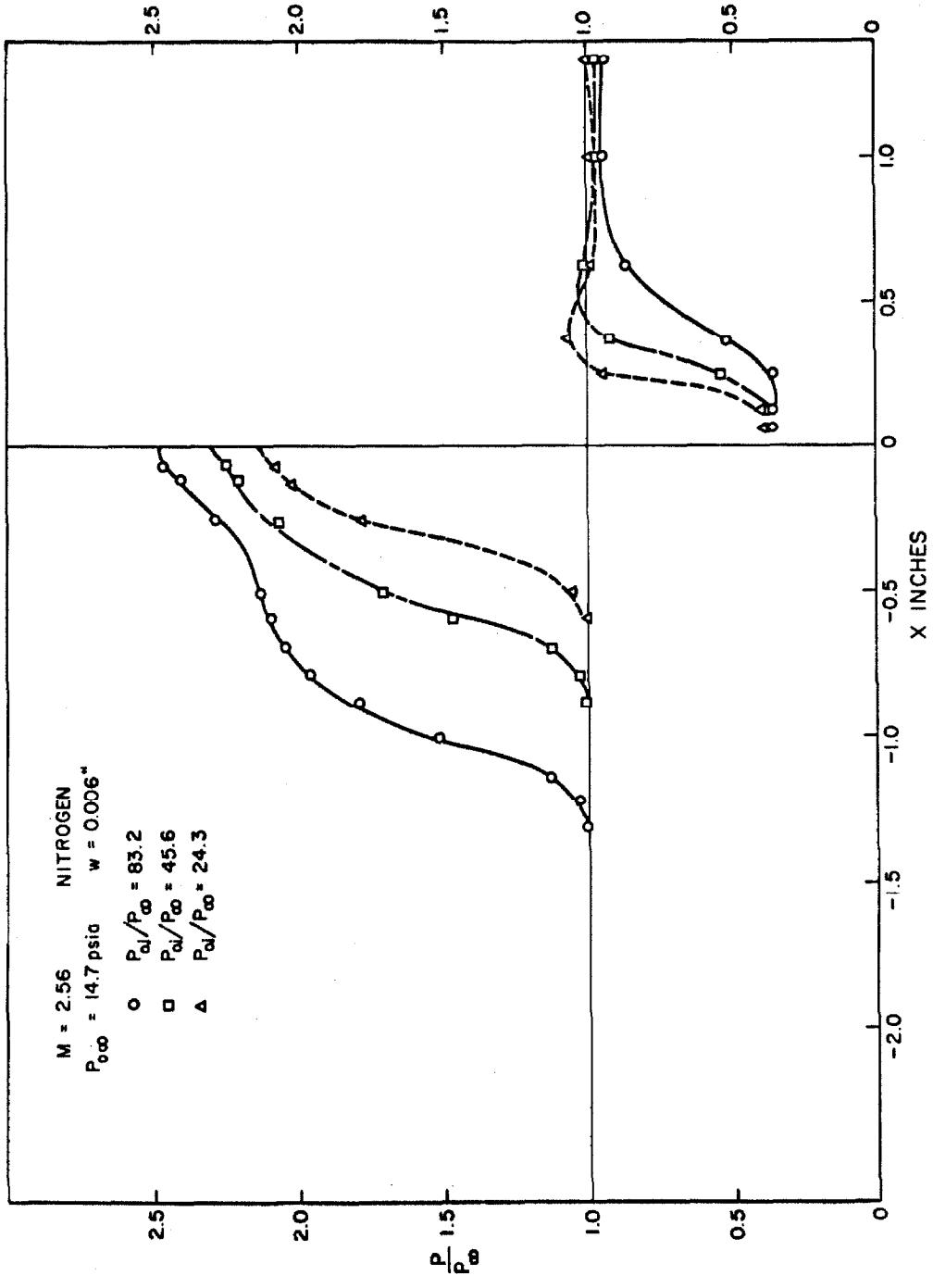

Figure 7. Pressure Distribution Caused by Nitrogen Injection Through the Wind Tunnel Wall at $M_\infty = 2.56$ and $Re = (2.35)(10)^5$ Per Inch.

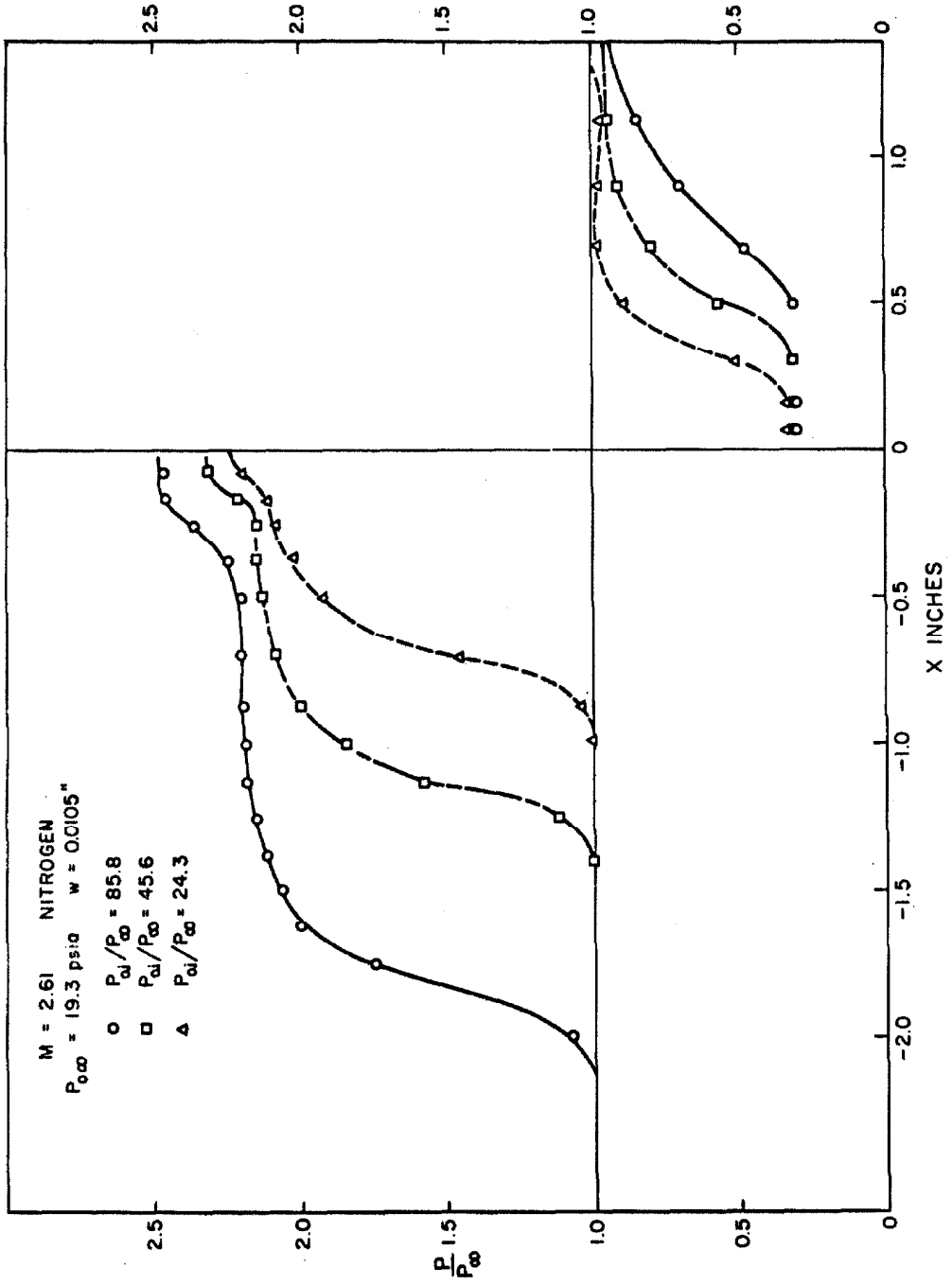

Figure 8. Pressure Distribution Caused by Nitrogen Injection Through a Slot in a Plate At $M_\infty = 2.61$ and $Re \approx 10^6$.

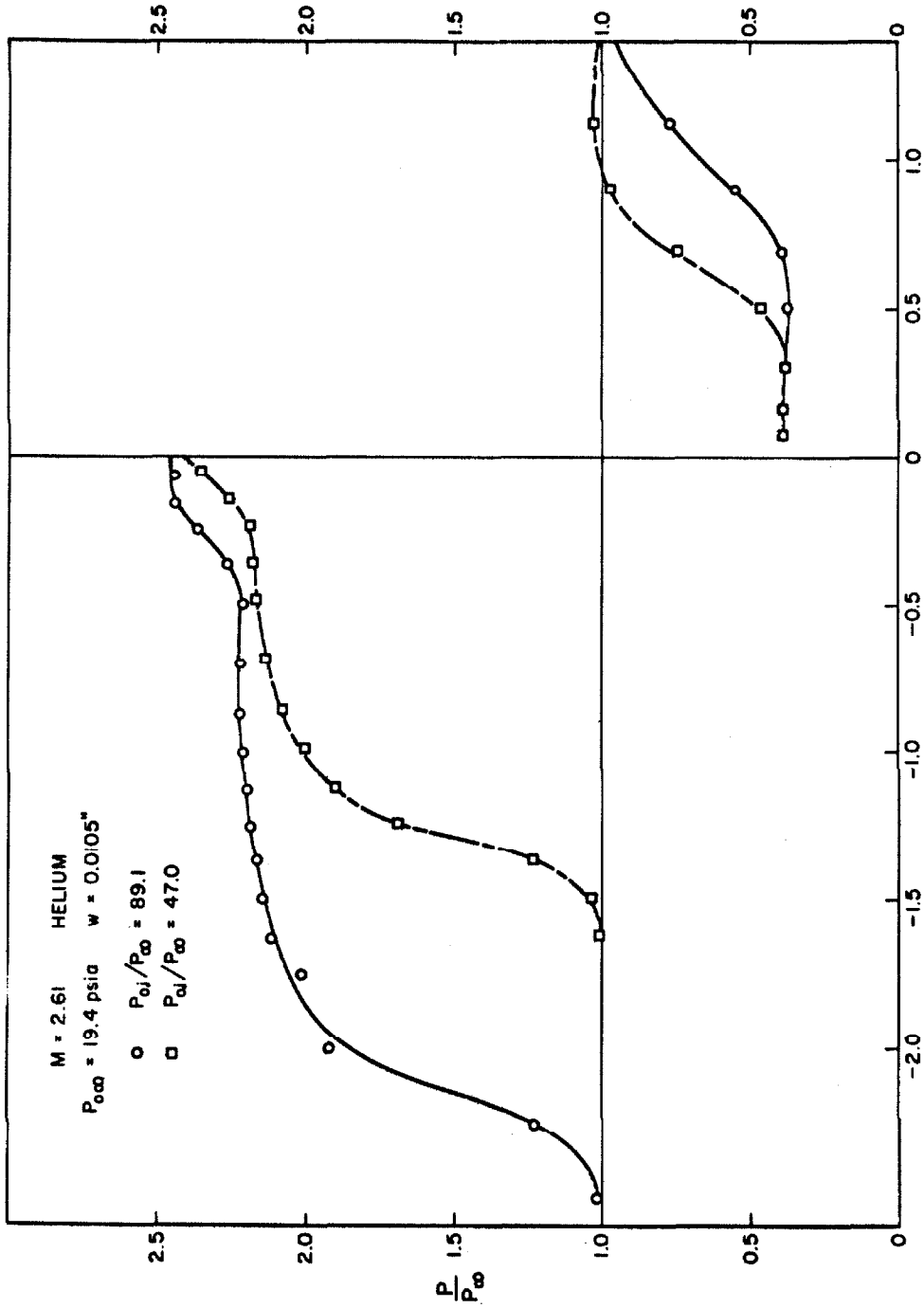

Figure 9. Pressure Distribution Caused by Helium Injection Through a Slot in a Plate at $M_{\infty} = 2.61$ and $Re \approx 10^6$.

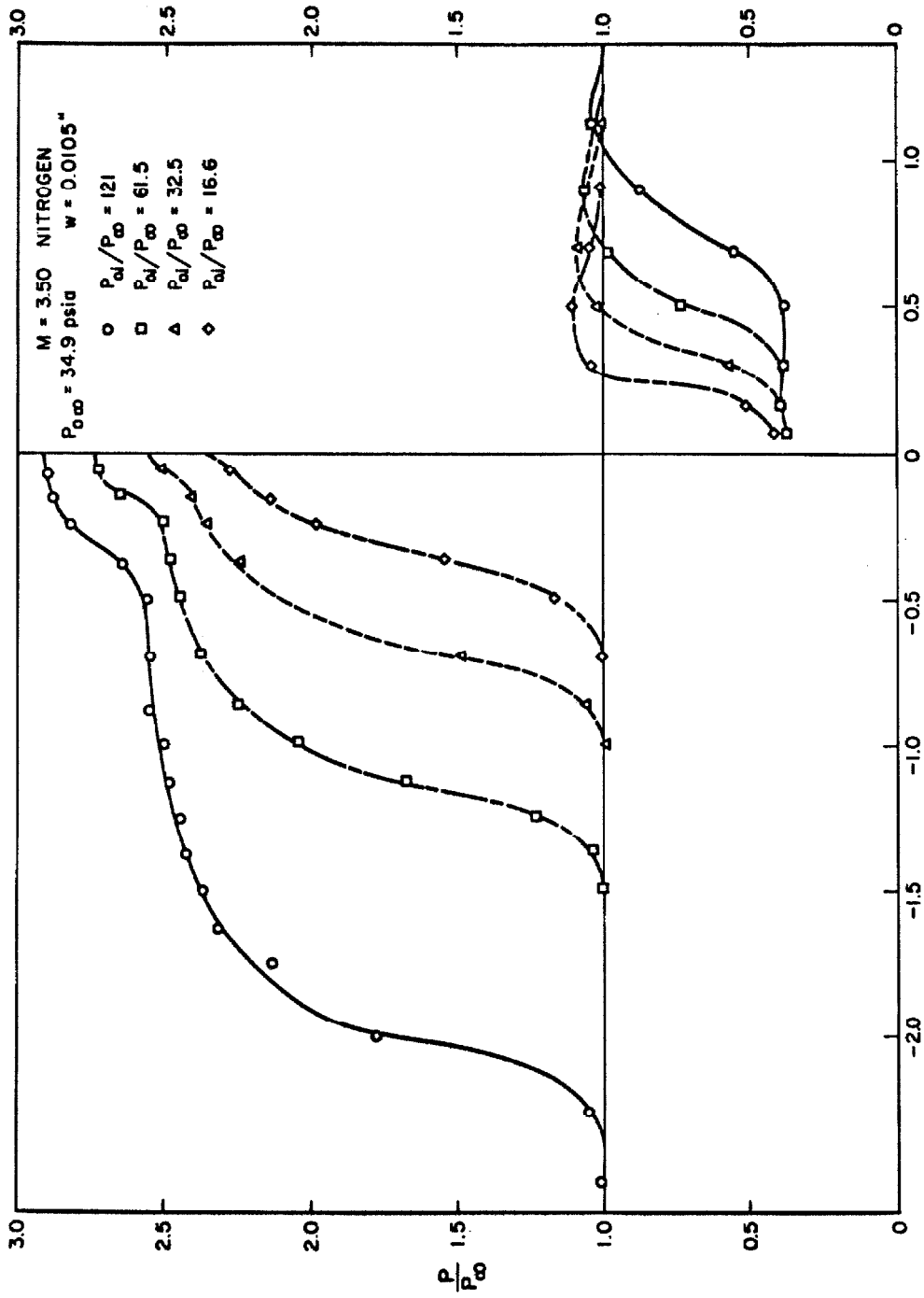

Figure 10. Pressure Distribution Caused by Nitrogen Injection Through a Slot in a Plate at $M_{\infty} = 3.50$ and $Re \approx 10^6$.

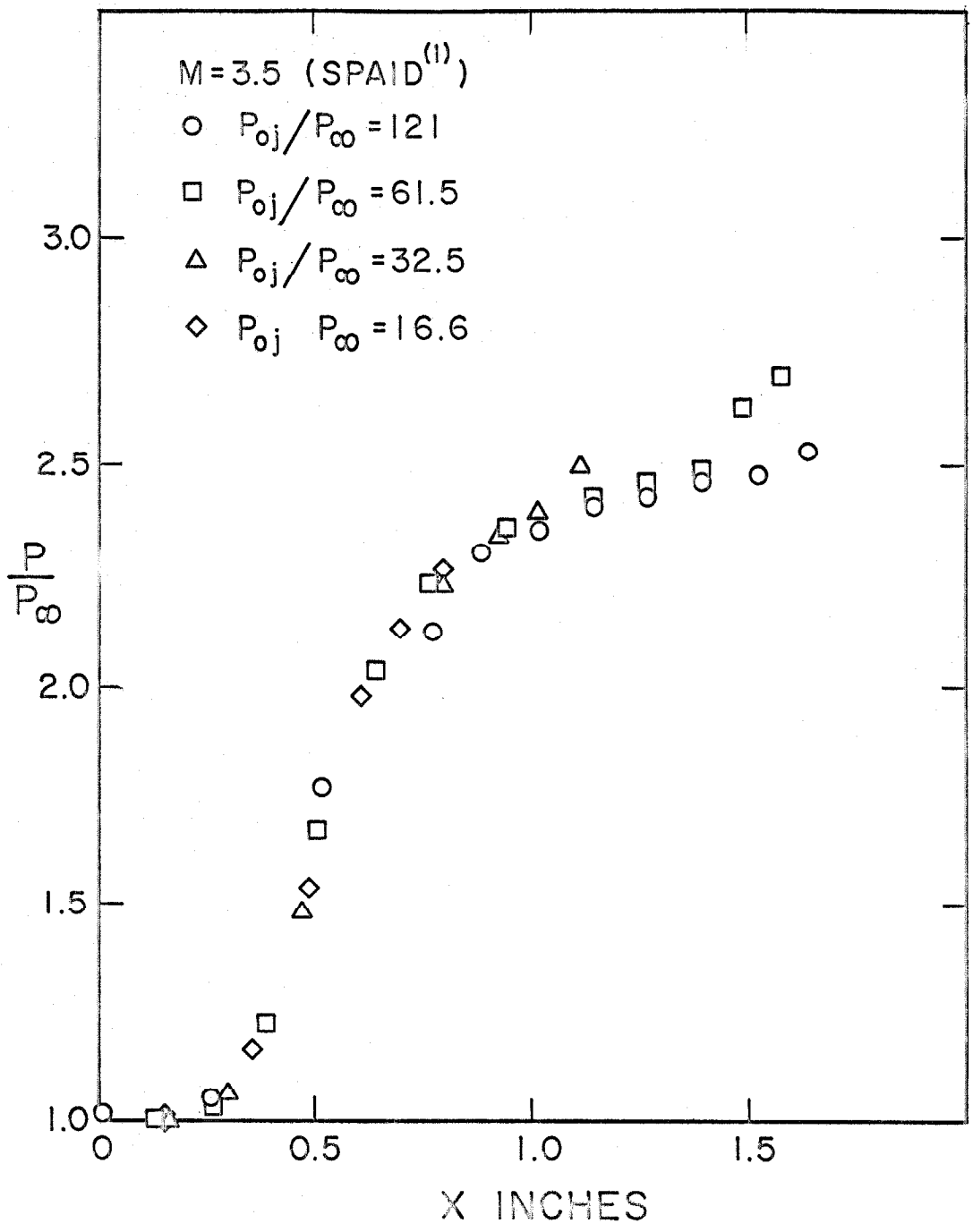

Figure 11. Similarity of the Pressure Fields at All Values of Injection Pressure for $M_\infty = 3.5$.

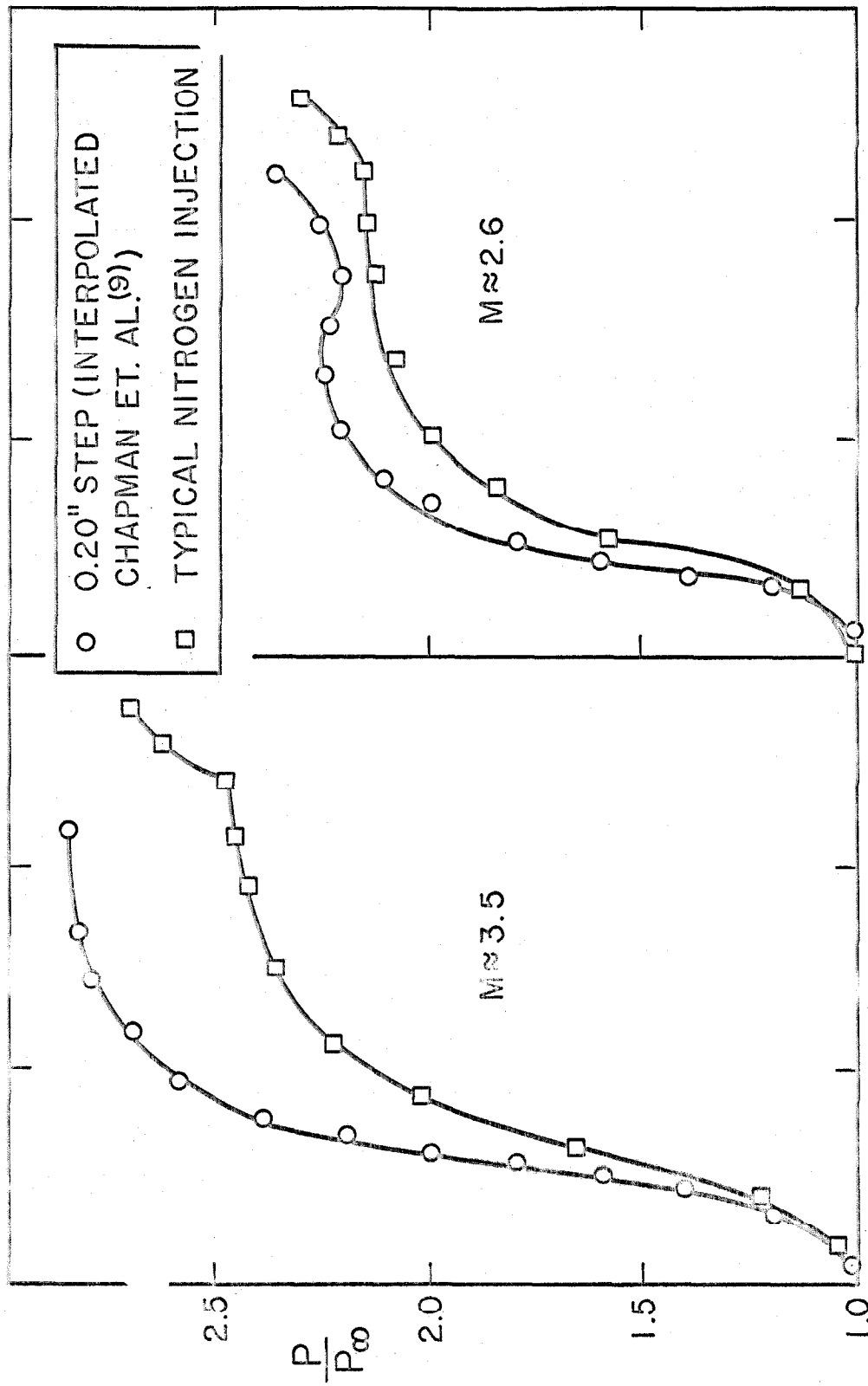

Figure 12. Comparison of Pressure Fields Created by Steps with Those Created by Injection Through a Slot.

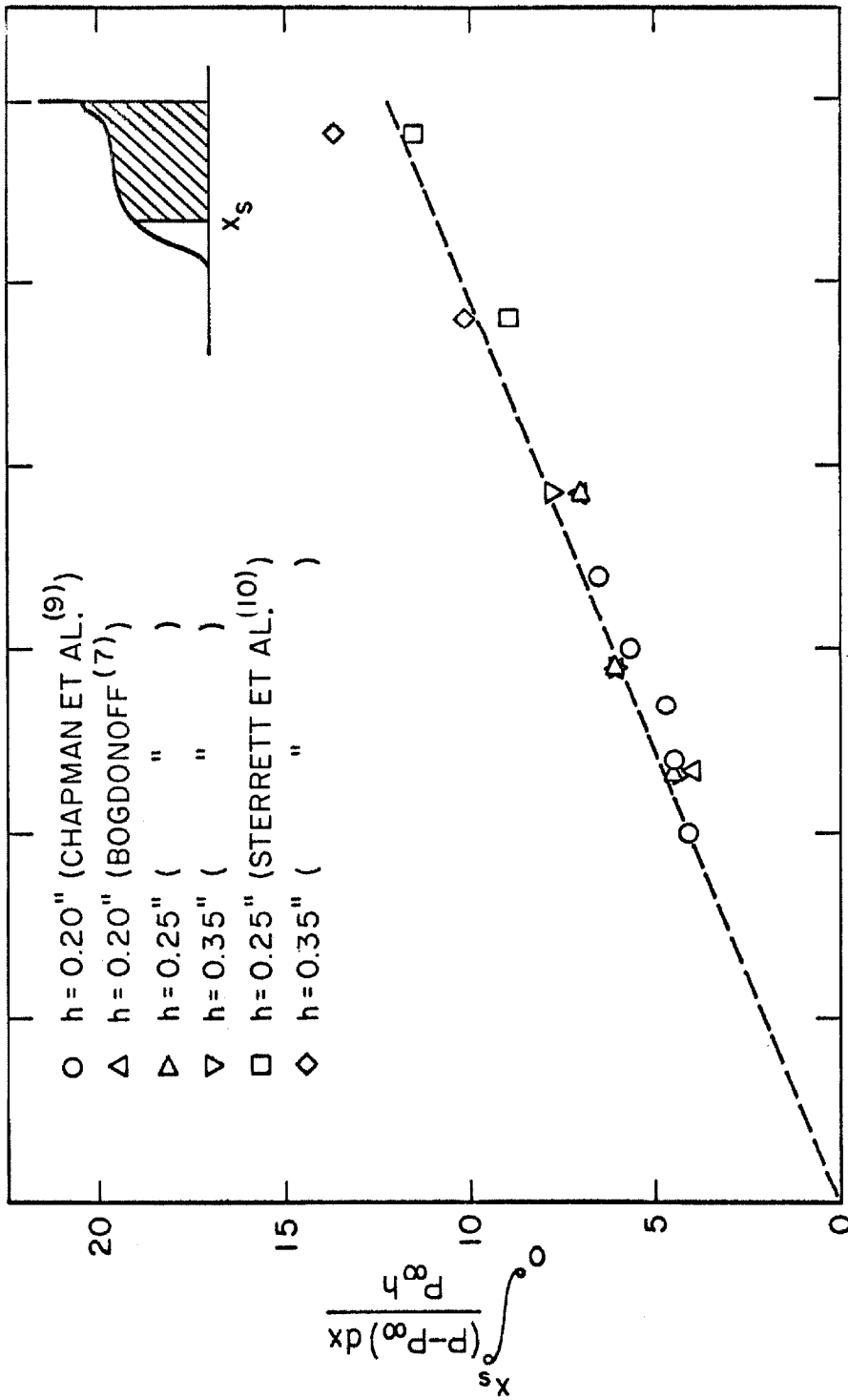

Figure 13. Mach Number Dependence of the Side Force Contributed by the Separated Region in Front of Forward-Facing Steps Larger than 0.20 Inches.

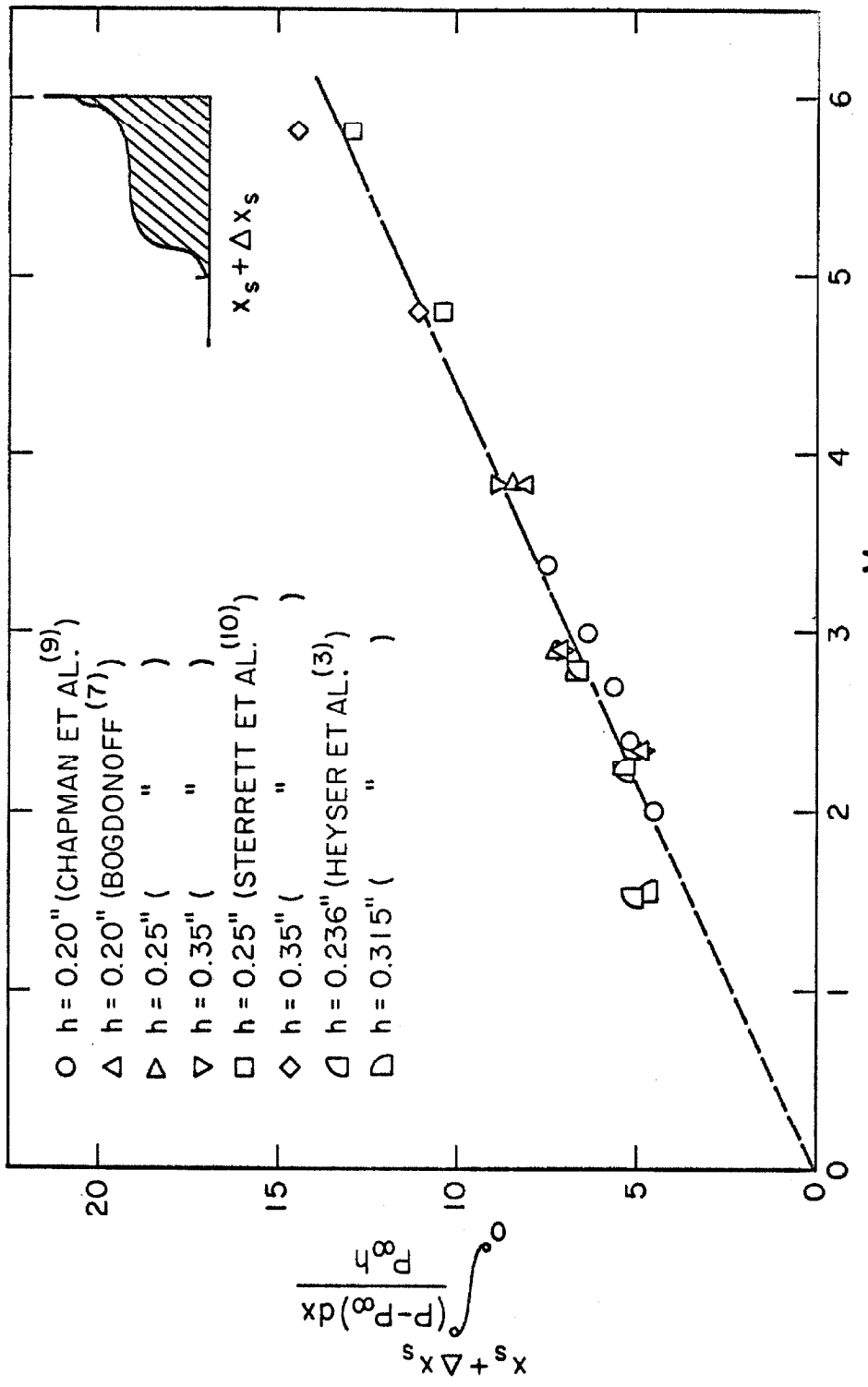

Figure 14. Mach Number Dependence of Total Side Force in Front of Forward-Facing Steps Greater than 0.20 Inches.

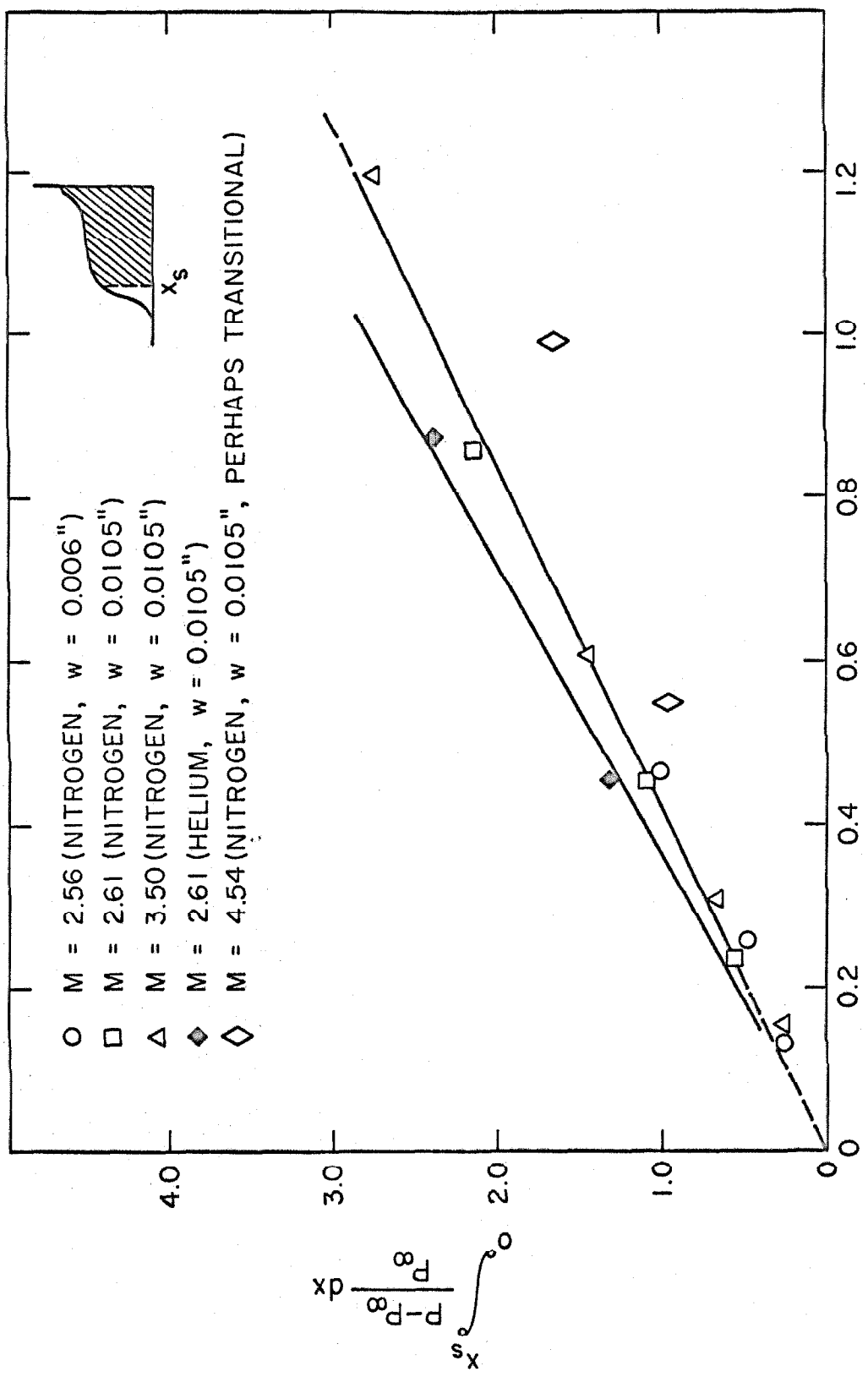

Figure 15: Side force, F_{s2} / P_{∞} , as a function of the momentum flux and γ of the injectant

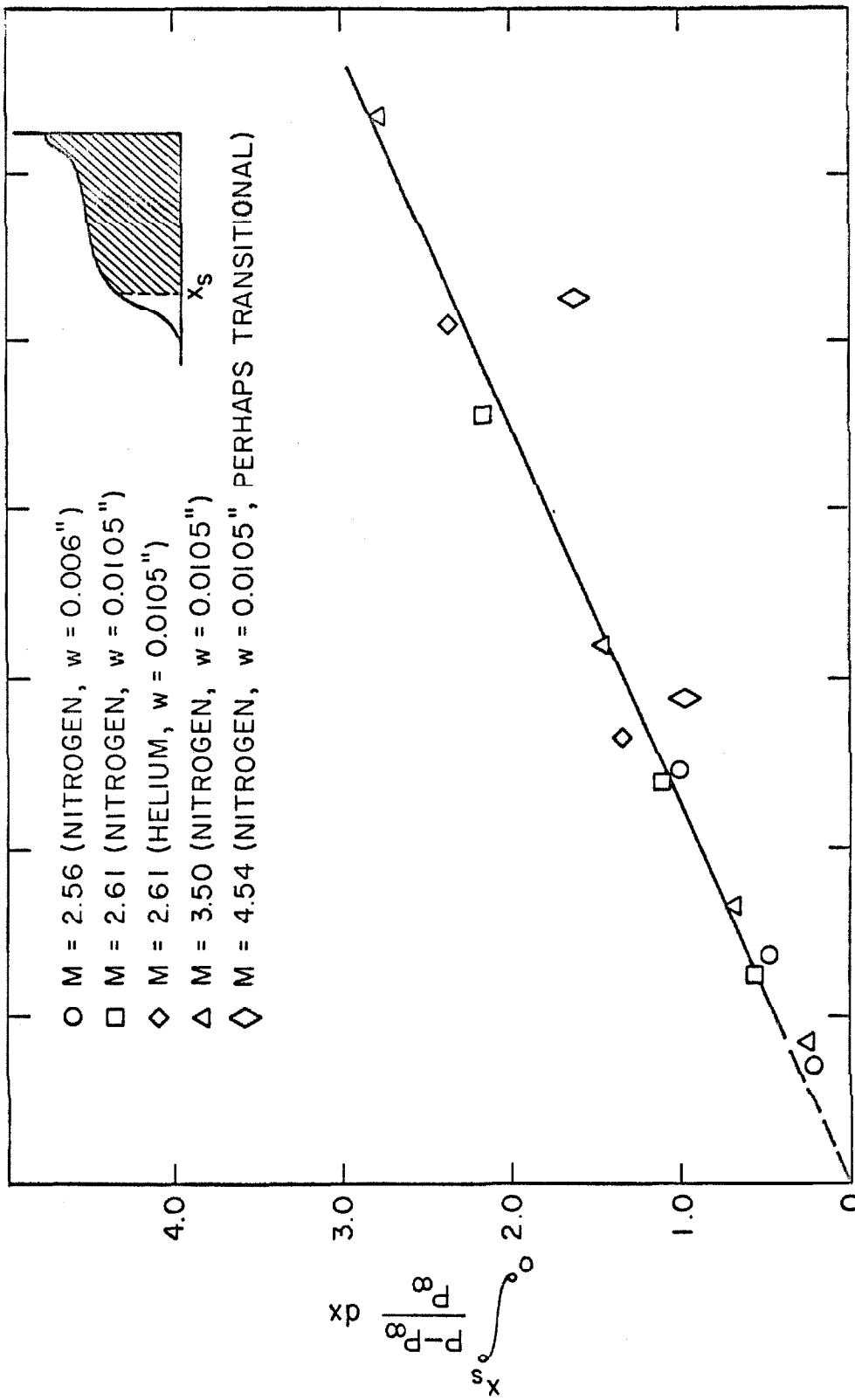

Figure 16: Side force, $F_{s\,2} / P_\infty$, as a function of the momentum flux of the injectant (equation 26).

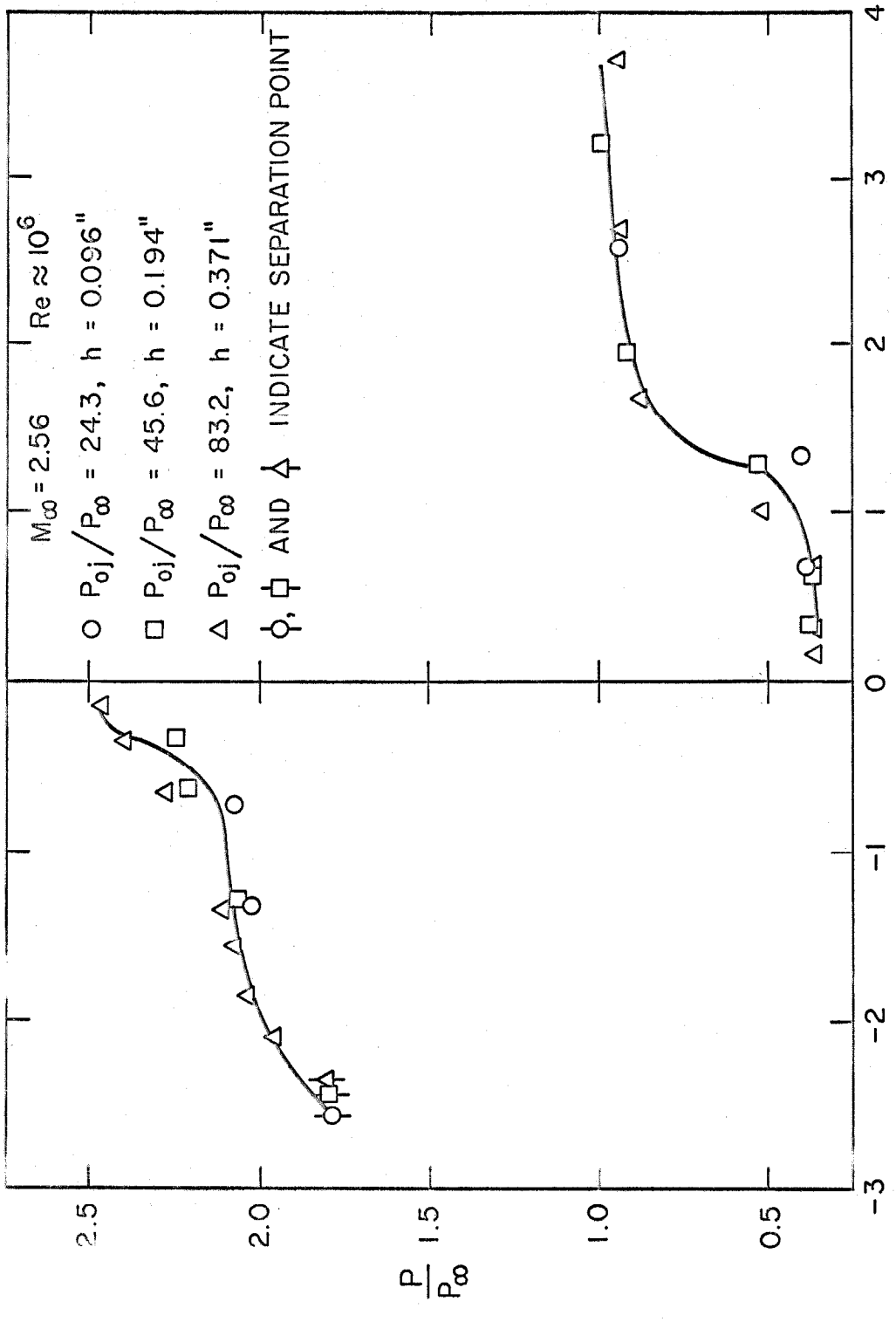

Figure 17. Pressure Field, Scaled with Equations (12) and (13), for Nitrogen Injection at $M_\infty = 2.56$.

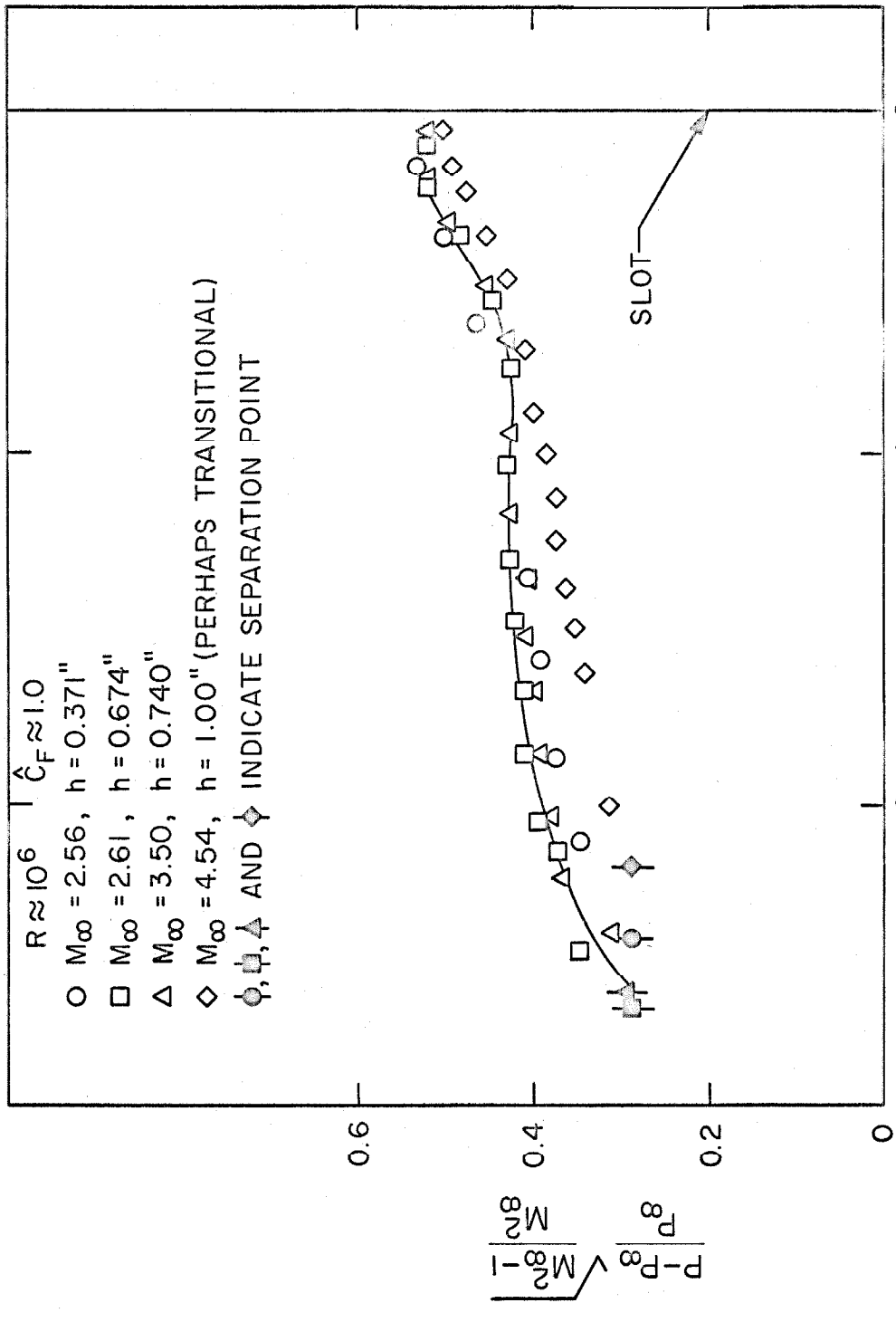

Figure 18. Pressure Fields Caused by Slot Injection Using Equations (11), (12), and (13) as Scaling Parameters.